



UNIVERSITY OF LEEDS

This is a repository copy of *Microfossils from the late Mesoproterozoic – early Neoproterozoic Atar/El Mreïti Group, Taoudeni Basin, Mauritania, northwestern Africa.*

White Rose Research Online URL for this paper:  
<http://eprints.whiterose.ac.uk/110731/>

Version: Accepted Version

---

**Article:**

Beghin, J, Storme, J-Y, Blanpied, C et al. (4 more authors) (2017) Microfossils from the late Mesoproterozoic – early Neoproterozoic Atar/El Mreïti Group, Taoudeni Basin, Mauritania, northwestern Africa. *Precambrian Research*, 291. pp. 63-82. ISSN 0301-9268

<https://doi.org/10.1016/j.precamres.2017.01.009>

---

© 2017 Published by Elsevier B.V. Licensed under the Creative Commons Attribution-NonCommercial-NoDerivatives 4.0 International  
<http://creativecommons.org/licenses/by-nc-nd/4.0/>

**Reuse**

Unless indicated otherwise, fulltext items are protected by copyright with all rights reserved. The copyright exception in section 29 of the Copyright, Designs and Patents Act 1988 allows the making of a single copy solely for the purpose of non-commercial research or private study within the limits of fair dealing. The publisher or other rights-holder may allow further reproduction and re-use of this version - refer to the White Rose Research Online record for this item. Where records identify the publisher as the copyright holder, users can verify any specific terms of use on the publisher's website.

**Takedown**

If you consider content in White Rose Research Online to be in breach of UK law, please notify us by emailing [eprints@whiterose.ac.uk](mailto:eprints@whiterose.ac.uk) including the URL of the record and the reason for the withdrawal request.



[eprints@whiterose.ac.uk](mailto:eprints@whiterose.ac.uk)  
<https://eprints.whiterose.ac.uk/>

## Accepted Manuscript

Microfossils from the late Mesoproterozoic – early Neoproterozoic Atar/El Mreïti Group, Taoudeni Basin, Mauritania, northwestern Africa

Jérémie Beghin, Jean-Yves Storme, Christian Blanpied, Nur Gueneli, Jochen J. Brocks, Simon W. Poulton, Emmanuelle J. Javaux

PII: S0301-9268(16)30133-4

DOI: <http://dx.doi.org/10.1016/j.precamres.2017.01.009>

Reference: PRECAM 4642

To appear in: *Precambrian Research*

Received Date: 9 May 2016

Revised Date: 30 November 2016

Accepted Date: 8 January 2017

Please cite this article as: J. Beghin, J.-Y. Storme, C. Blanpied, N. Gueneli, J.J. Brocks, S.W. Poulton, E.J. Javaux, Microfossils from the late Mesoproterozoic – early Neoproterozoic Atar/El Mreïti Group, Taoudeni Basin, Mauritania, northwestern Africa, *Precambrian Research* (2017), doi: <http://dx.doi.org/10.1016/j.precamres.2017.01.009>

This is a PDF file of an unedited manuscript that has been accepted for publication. As a service to our customers we are providing this early version of the manuscript. The manuscript will undergo copyediting, typesetting, and review of the resulting proof before it is published in its final form. Please note that during the production process errors may be discovered which could affect the content, and all legal disclaimers that apply to the journal pertain.



1 **Microfossils from the late Mesoproterozoic – early Neoproterozoic Atar/EI**  
2 **Mreïti Group, Taoudeni Basin, Mauritania, northwestern Africa**

3 Jérémie Beghin<sup>1\*</sup>, Jean-Yves Storme<sup>1</sup>, Christian Blanpied<sup>2</sup>, Nur Gueneli<sup>3</sup>, Jochen J.  
4 Brocks<sup>3</sup>, Simon W. Poulton<sup>4</sup> and Emmanuelle J. Javaux<sup>1\*</sup>

5 <sup>1</sup>Department of Geology, UR GEOLOGY, University of Liège, Liège, Belgium.

6 \*Corresponding authors: [jbeghin@ulg.ac.be](mailto:jbeghin@ulg.ac.be) (Jérémie Beghin), [ej.javaux@ulg.ac.be](mailto:ej.javaux@ulg.ac.be)  
7 (Emmanuelle Javaux). Quartier Agora, Bâtiment B18, Allée du six août, 14, B-4000  
8 Liège, Belgium)

9 <sup>2</sup>TOTAL, Projets Nouveaux, Paris, France

10 <sup>3</sup>Research School of Earth Sciences, The Australian National University, Canberra,  
11 ACT 2601, Australia

12 <sup>4</sup>School of Earth and Environment, University of Leeds, Leeds, LS2 9JT, United  
13 Kingdom

14 **Abstract**  
15

16 The well-preserved Meso-Neoproterozoic shallow marine succession of the  
17 Atar/EI Mreïti Group, in the Taoudeni Basin, Mauritania, offers a unique opportunity to  
18 investigate the mid-Proterozoic eukaryotic record in Western Africa. Previous  
19 investigations focused on stromatolites, biomarkers, chemostratigraphy and  
20 palaeoredox conditions. However, only a very modest diversity of organic-walled  
21 microfossils (acritarchs) has been documented. Here, we present a new, exquisitely  
22 well-preserved and morphologically diverse assemblage of organic-walled  
23 microfossils from three cores drilled through the Atar/EI Mreïti Group. A total of 48

24 distinct entities including 11 unambiguous eukaryotes (ornamented and process-  
25 bearing acritarchs), and 37 taxonomically unresolved taxa (including 9 possible  
26 eukaryotes, 6 probable prokaryotes, and 22 other prokaryotic or eukaryotic taxa)  
27 were observed. Black shales preserve locally abundant fragments of benthic  
28 microbial mats. We also document one of the oldest records of *Leiosphaeridia*  
29 *kulgunica*, a species showing a pylome interpreted as a sophisticated circular  
30 excystment structure, and one of the oldest records of *Trachyhystriosphera*  
31 *aimika* and *T. botula*, two distinctive process-bearing acritarchs present in well-dated  
32 1.1 Ga formations at the base of the succession. The general assemblage  
33 composition and the presence of three possible index fossils (*A. tetragonala*, *S.*  
34 *segmentata* and *T. aimika*) support a late Mesoproterozoic to early Neoproterozoic  
35 (Tonian) age for the Atar/El Mreïti Group, consistent with published lithostratigraphy,  
36 chemostratigraphy and geochronology. This study provides the first evidence for a  
37 moderately diverse eukaryotic life, at least 1.1 billion years ago in Western Africa.  
38 Comparison with coeval worldwide assemblages indicate that a broadly similar  
39 microbial biosphere inhabited (generally redox-stratified) oceans, placing better time  
40 constraints on early eukaryote palaeogeography and biostratigraphy.

#### 41 **Keywords**

42 Mesoproterozoic. Neoproterozoic (Tonian). Acritarchs. Microfossils. Eukaryotes.  
43 Biostratigraphy. Palaeogeography.

#### 44 **1. Introduction**

45 Mid-Proterozoic organic-walled microfossil assemblages seem to be broadly  
46 similar worldwide, despite some differences possibly related to redox conditions (e.g.  
47 Sergeev et al., 2016), facies preservation, sample preparation, lack of recent detailed

48 taxonomic revision, or sampling bias, but similarities may suggest oceanic  
49 connections between most basins. However, global comparisons are not possible  
50 while in some areas of the Proterozoic world, such as the West African Craton  
51 (WAC), the microfossil record is still poorly documented. Previous palaeobiological  
52 investigations of the Taoudeni Basin, in northwest Africa (Fig. 1), have mainly  
53 focused on stromatolites (Bertrand-Sarfati and Moussine-Pouchkine, 1985, 1988;  
54 Kah et al., 2009) and more recently on biomarkers (Blumenberg et al., 2012; Gueneli  
55 et al., 2012, 2015), but there has been limited discussion on microfossils, mostly on  
56 unornamented ubiquitous and poorly diverse acritarchs (Amard, 1986; Ivanovskaya  
57 et al., 1980; Lottaroli et al., 2009; Blumenberg et al., 2012).

58 In contrast, extensive work has focused on the Taoudeni Basin sedimentology  
59 (Lahondère et al., 2003; Kah et al., 2012), geochronology (Clauer, 1976, 1981;  
60 Clauer et al., 1982; Clauer and Deynoux, 1987; Rooney et al., 2010),  
61 chemostratigraphy (Kah et al., 2012; Gilleaudeau and Kah, 2013a), and palaeoredox  
62 conditions (Gilleaudeau and Kah, 2013b, 2015). Relatively new Re-Os  
63 geochronologic dating (Rooney et al., 2010) and chemostratigraphy (Fairchild et al.,  
64 1990; Teal and Kah, 2005; Kah et al., 2009, 2012) suggest a late Mesoproterozoic  
65 (~1.1 Ga) age for the stratigraphically lower deposits of the Atar/El Mreïti Group in  
66 the Taoudeni Basin (Fig. 2).

67 Here we report on a new diverse assemblage of organic-walled microfossils  
68 preserved in late Mesoproterozoic-early Neoproterozoic shales of the Atar/El Mreïti  
69 Group in the Taoudeni Basin, Mauritania. The Mesoproterozoic-Neoproterozoic  
70 transition is increasingly recognized as a key interval in both planetary and eukaryotic  
71 evolution. The discovery of a number of unambiguously eukaryotic fossils, in addition  
72 to taxa unassigned to a particular domain, improves their known stratigraphic and

73 palaeogeographic distribution and more broadly, the pattern of early eukaryote  
74 diversification and evolution.

## 75 **2. Geological setting of the Taoudeni Basin**

76 The Taoudeni Basin (Fig. 1), northwest Africa, is the largest Proterozoic and  
77 Palaeozoic sedimentary basin (intra-cratonic platform) in Africa (>1,750,000 km<sup>2</sup>), and  
78 extends from Mauritania to northern Mali and western Algeria (Lahondère et al.,  
79 2003; Gilleaudeau and Kah, 2013a, 2013b, 2015). This large depression in the  
80 continental platform contains kilometer-thick sedimentary deposits (up to 1,300 m) of  
81 gently dipping (<1°), unmetamorphosed and undeformed Proterozoic to Palaeozoic  
82 strata, which are overlain in the basin's centre by a thin Meso-Cenozoic cover. The  
83 Proterozoic and Phanerozoic strata unconformably overlie an Archean-  
84 Palaeoproterozoic basement (Lahondère et al., 2003; Rooney et al., 2010; Kah et al.,  
85 2012; Gilleaudeau and Kah, 2013a, 2013b, 2015).

86 In total, four Megasequences or Supergroups bound by craton-scale  
87 unconformities are recognized (Trompette, 1973; Trompette and Carozzi, 1994;  
88 Deynoux et al., 2006). Supergroup 1 (this study) or Hodh (Fig. 2) rests upon the  
89 metamorphic and granitic basement (Lahondère et al., 2003). The type section for  
90 the Taoudeni Basin was previously described in the Adrar region of the Mauritanian  
91 section, in the western part of the basin (Trompette, 1973). Supergroup 1 is divided  
92 into three unconformable groups (Lahondère et al., 2003), which correlate between  
93 the Adrar region and the north-central edge of the basin (in the Hank and Khatt  
94 areas). The Char Group in the Adrar region corresponds to the Douik Group in the  
95 north-central region, the Atar Group to the El Mreïti Group (studied here, Fig. 3), and

96 the Assabet el Hassiane Group in the west to the Cheikhia Group in the east (Figs 1  
97 and 2).

98 These groups are subdivided into units (Trompette, 1973) or formations  
99 (Lahondère et al., 2003). The 0-300 m thick Char Group - divided into Unit I-1 and  
100 Unit I-2 - comprises fluvial sandstones, coastal aeolian deposits and shallow-marine  
101 siltstones and shales (Figs 1 and 2; Benan and Deynoux, 1998; Kah et al., 2012).  
102 The Char Group was deposited during active extension of the basement  
103 (Gilleaudeau and Kah, 2015), possibly related to the opening of the Brasiliano Ocean  
104 rather than to the formation or break-up of Rodinia (Rooney et al., 2010). The basin-  
105 wide unconformity between the Char Group and the overlying Atar Group is of an  
106 unknown duration (Benan and Deynoux, 1998; Deynoux et al., 2006). The overlying  
107 Atar Group comprises about 800 m of sedimentary rocks, starting with a sandy fluvial  
108 to estuarine basal part (Unit I-3), followed by a succession of interbedded  
109 stromatolitic carbonates and shales (Units I-4 to I-12; Figs 1 and 2) deposited in a  
110 shallow marine environment (craton-wide flooding of epeiric/pericratonic sea;  
111 Trompette, 1973; Trompette and Carozzi 1994; Bertrand-Sarfati and Moussine-  
112 Pouchkine, 1985, 1999; Kah et al., 2012; Gilleaudeau and Kah, 2013a, 2013b).  
113 Resting above an erosional surface, the 300-400 m thick Assabet el  
114 Hassiane/Cheikhia Group (Units I-13 to I-18) comprises fine-grained marine  
115 sandstone, siltstone and shales deposited in a range of shallow to deep marine  
116 environments (see Figs 1 and 2; Trompette and Carozzi, 1994; Moussine-Pouchkine  
117 and Bertrand-Sarfati, 1997; Kah et al., 2012). Supergroup 1 is unconformably overlain  
118 by tillites and cap dolostones of the Jbéliat Group, which forms the basal part of  
119 Supergroup 2 (Figs 1 and 2; Lahondère et al., 2003).

### 120 3. Age of the Atar/El Mreïti Group

121 The age of the Atar/El Mreïti Group was first poorly constrained by Rb-Sr  
122 geochronology (Clauer, 1976, 1981; Clauer et al., 1982) performed on glauconite and  
123 illite in shaley intervals (Fig. 2). The Atar/El Mreïti Group was constrained between  
124  $998 \pm 32$  Ma (Unit I-2) to  $> 694$  Ma for the Assabet el Hassiane/Cheikhia Group  
125 (Units I-15 and I-16) and 630-595 Ma for the glacial Jbéliat Group (Clauer and  
126 Deynoux, 1987; Fig. 2). Most formations in the Atar/El Mreïti Group were constrained  
127 by a single age (Fig. 2). However, these Rb-Sr ages clearly represent diagenetic  
128 mineralization (Kah et al., 2009), possibly due to the Pan African collision (Rooney et  
129 al., 2010). The glacial deposits of the Jbéliat Group unconformably overlying the  
130 Assabet el Hassiane/Cheikhia Group are interpreted as late Cryogenian or Marinoan  
131 correlative based on lithology and chemostratigraphy on  $\delta^{13}\text{C}_{\text{carb}}$  and  $\delta^{18}\text{O}_{\text{carb}}$  from  
132 cap carbonates or dolostones (Álvaro et al., 2007; Shields et al., 2007) and  $^{87}\text{Sr}/^{86}\text{Sr}$   
133 ratio and  $\delta^{34}\text{S}$  from barite (Shields et al., 2007). Strontium isotope compositions from  
134 geographically distant locations within the Taoudeni Basin range from 0.70773 to  
135 0.70814 and support the early Ediacaran age of the Jbéliat barite-bearing cap  
136 dolostones overlying the Jbéliat Group tillite (Shields et al., 2007; Halverson et al.,  
137 2007; 2010). This interpretation is also supported by dates from two volcanic tuffs in  
138 the Téniaourri Group, directly overlying the glacial Jbéliat Group, which have been  
139 dated at  $609.7 \pm 5.5$  Ma (U/Pb zircon) and  $604 \pm 6$  Ma (U/Pb SHRIMP) (Lahondère et  
140 al., 2005; Shields et al., 2007).

141 Rooney et al. (2010) performed Re-Os geochronology on organic-rich black  
142 shales from formations close to the base of the stratigraphy (in drill cores S1 and S2:  
143 same as this study; Fig. 1). These drill cores gave an age of  $1107 \pm 12$  Ma (139.45 to  
144 143.82 m depth; Tourist Formation) and  $1109 \pm 22$  Ma (206.70 to 207.60 m depth;  
145 En Nesoar Formation) for core S2 (Figs 2 and 3), and  $1105 \pm 37$  Ma (73.15 to 89.50



146 m depth; Tourist Formation) for core S1 (Rooney et al., 2010). The Re-Os ages  
147 obtained on these cores are similar, despite contact metamorphism by doleritic sills  
148 or dikes affecting one of them (S1) (Fig. 1).

149 Based on carbon isotope chemostratigraphy, the Atar/El Mreïti Group may be as  
150 old as ~1200 Ma (Kah et al., 2009, 2012). Carbon isotope data from the Atar/El Mreïti  
151 Group (Fairchild et al., 1990; Teal and Kah, 2005) revealed moderately positive  
152  $\delta^{13}\text{C}_{\text{carb}}$  values near +4‰, with several distinct negative excursions to nearly -2.5‰  
153 (Kah et al., 2009; 2012). This range of  $\delta^{13}\text{C}_{\text{carb}}$  values differs from the positive values  
154 ( $\delta^{13}\text{C}_{\text{carb}} > +5\text{‰}$ ) recorded in post-850 Ma Neoproterozoic (Kaufman and Knoll, 1995;  
155 Knoll, 2000; Halverson et al., 2005, 2010; Macdonald et al., 2010) and in early  
156 Neoproterozoic strata (Knoll et al., 1995; Bartley et al., 2001), but are similar to the  
157 isotopic patterns preserved globally in mid to late Mesoproterozoic strata after 1.25  
158 Ga (Bartley et al., 2001), in the Bylot Supergroup and Dismal Lake Group, Arctic  
159 Canada (Kah et al., 1999; Frank et al., 2003), the Anabar Massif, northwestern  
160 Siberia (Knoll et al., 1995), and the southern Urals, Russia (Bartley et al., 2007).

#### 161 **4. Material and methods**

162 Four cores were drilled at the northern margin of the Taoudeni Basin by the oil  
163 company TOTAL S. A. in 2004 (Rooney et al., 2010). The cores were named from the  
164 east to the west, S1, S2, S3 and S4 (Fig. 1). S1 was not studied here because of  
165 contact metamorphism due to dolerite intrusions (Fig. 1). S2 was sampled (by E.J. J.)  
166 in 2006 in TOTAL S.A. laboratory and is described here in detail (Fig. 3). All S3  
167 samples come from the Aguelte el Mabha Formation (laminated black and grey  
168 shales). Samples from S4 come from the following three units: Unit I-3/Khatt  
169 Formation, Unit I-4/En Nesoar Formation and Unit I-5/Tourist and/or Aguelte el Mabha

170 formations; all S4 samples are dark grey or black shales. In core S2, we recognize  
171 five formations through the El Mreïti Group (Fig. 3), with two formations (En Nesoar  
172 and Tourist formations) chronostratigraphically constrained by Rooney et al. (2010)  
173 (Fig. 2 and section 3).

174 A total of 166 samples (S2 = 143, S3 = 5 and S4 = 18) were analyzed for  
175 micropalaeontology. Kerogen extraction (acritarchs, other acid-insoluble microfossils  
176 and organic remains) from rock samples followed the preparation procedure  
177 described by Grey (1999), avoiding centrifugation or mechanical shocks that could  
178 damage fragile fossilized forms and oxidation that could alter kerogenous wall  
179 chemistry and color. Palynological slides were scanned under 100, 200, 400, and  
180 1000× magnification with a transmitted light microscope (Carl Zeiss Primo Star).  
181 Each specimen illustrated here was localized with coordinates using an England  
182 Finder graticule (Pyser-SGI), imaged with a digital camera Carl Zeiss Axiocam MRc5  
183 on a transmitted light microscope (Carl Zeiss Axio Imager A1m), and measured using  
184 eyepiece graticule or the software AxioVision. All palynological slides are stored in  
185 the collections of the Palaeobiogeology - Palaeobotany - Palaeopalynology  
186 laboratory, Geology Department, UR GEOLOGY, at the University of Liège, Belgium.  
187 The species identified in the assemblage are listed in Table 1 and illustrated in  
188 alphabetical order in Plates 1-4. The stratigraphic occurrence of each species is  
189 reported in the Suppl. Fig. 1A-B (S2 core), Suppl. Fig. 2 (S3 core) and Suppl. Fig. 3  
190 (S4 core).

## 191 5. Previous palaeontological investigations of the Taoudeni Basin

192 The Taoudeni Basin is known to preserve remarkable stromatolites (*Conophyton-*  
193 *Jacutophyton* and *Baicalia* associations) in Mauritania, which were extensively

194 studied by Bertrand-Sarfati (1972) and Bertrand-Sarfati and Moussine-Pouchkine  
195 (1985 and 1988). Relationships between these stromatolites and sea-level changes  
196 have been characterized by Kah et al. (2009). A small assemblage of smooth-walled  
197 acritarchs, colonies of small vesicles, and simple filamentous microfossils was  
198 previously reported in early studies conducted on outcrop and subsurface samples in  
199 the Adrar region on the northwestern part of the basin (Ivanovskaya et al., 1980;  
200 Amard, 1986; Lottaroli et al., 2009; Blumenberg et al., 2012). Many of the reported  
201 taxa (Suppl. Table 1) have since been synonymized (Jankauskas et al., 1989) or  
202 have been judged by the current authors as too poorly preserved (or illustrated) for  
203 identification. Ivanovskaya et al. (1980) reported 10 species, revised to two species  
204 of chagrinated sphaeromorphs according to Amard (1986), although taphonomic  
205 alteration of simple leiospheres cannot be excluded based on available illustrations.  
206 Amard (1986) reported 20 acritarch species from macerated samples, revised to 12  
207 based on available descriptions (Suppl. Table 1), from a water well of the Atar Group  
208 (Unit I-5/Tod/Tourist and/or Aguel el Mabha formations). This assemblage was  
209 interpreted as late Riphean/early Neoproterozoic (~1-0.65 Ga) based on similarities  
210 with the Riphean of USSR and Northern Europe (Amard, 1984, 1986). Lottaroli et al.  
211 (2009) reported 12 species, revised to 10 based on available illustrations or  
212 descriptions (Suppl. Table 1), from macerated well-preserved samples of the core  
213 Abolag 1, and also gave this assemblage a Tonian-Cryogenian age (~ 1-0.65 Ga).  
214 Blumenberg et al. (2012) reported only abundant isolated or clustered moderately  
215 well preserved smooth-walled sphaeromorphs from one macerated sample from  
216 black shale of the Tourist Formation (El Mreïti Group).

217 Biomarkers extracted from black shales of the Tourist Formation, El Mreïti Group,  
218 suggested the presence of microbial communities dominated by cyanobacteria and

219 anoxygenic photosynthetic bacteria, but no steranes indicative of eukaryotes were  
220 found (Blumenberg et al., 2012). Gueneli et al. (2012, 2015) described bacterial  
221 communities, but biomarkers diagnostic of crown group eukaryotes were either below  
222 detection limit or absent.

## 223 **6. Diversity of the Atar/El Mreiti Group microfossil assemblage**

224 Our study of a large suite of shale samples revealed a larger diversity than  
225 previously reported for the Atar/El Mreiti Group (Table 1, Pl. 1-4). Out of the 166  
226 sample analyzed, 129 revealed microfossils (Fig. 3). Overall, 48 distinct entities are  
227 recognized in the assemblage, including 46 identified species of organic-walled  
228 microfossils and 2 unnamed forms (A and B). Locally abundant fragments of benthic  
229 microbial mats with embedded pyritized filaments were also observed in black  
230 shales. Their detailed stratigraphic occurrences through the cores are summarized in  
231 supplementary figures (1A-B, 2, 3).

### 232 **Smooth-walled spheroidal acritarchs**

233 As in most Proterozoic fossiliferous shales, the most common acritarchs are  
234 smooth-walled leiospheres: abundant *Leiosphaeridia crassa* (Pl. 2c-d), and lesser  
235 amount of *L. jacutica* (Pl. 2e), *L. minutissima* (Pl. 2g-h) and *L. tenuissima* (Pl. 2j).  
236 Other smooth-walled sphaeromorphs include two specimens of *Chuarina circularis* (Pl.  
237 1h), a large dark-brown nearly opaque thick-walled spheroidal vesicle (440 and 810  
238  $\mu\text{m}$  in diameter), and a few specimens of *L. ternata* (Pl. 2k), a dark brown to opaque  
239 smooth-walled spheroidal vesicle, 17.5–32.5  $\mu\text{m}$  in diameter, showing radial fractures  
240 starting from the periphery. The wall of this latter species is clearly rigid and brittle  
241 (i.e. non-flexible) when subjected to mechanical compressive stress during

242 sedimentary compaction, giving rise to the characteristic but taphonomic radial  
243 fractures.

244 A small population of smooth-walled leiospheres 35-52.5  $\mu\text{m}$  in diameter  
245 (mean = 44.2  $\mu\text{m}$ , SD = 5.9  $\mu\text{m}$ , n = 9) and characterized by the presence of a 12.5-  
246 21.3  $\mu\text{m}$  in diameter circular opening, are interpreted as *L. kulgunica* (Pl. 2f). The  
247 regular morphology of the opening limited by a smooth unornamented rim suggests  
248 an excystment structure: a pylome. The Taoudeni population fits in the range of  
249 diameters reported by Jankauskas et al. in 1989 (10-15 to 30-35  $\mu\text{m}$ , up to 65  $\mu\text{m}$ ),  
250 although generally larger and showing larger pylome diameters (8-12  $\mu\text{m}$  in  
251 Jankauskas et al., 1989), that are always over 25% (~30-40%) of the vesicle  
252 diameter (macro-pylome). No operculum was preserved. It is not clear at this point if  
253 these differences warrant the description of a new species or are part of the  
254 variability of *L. kulgunica*. Butterfield et al. (1994, p. 43) placed *L. kulgunica* in the  
255 genus *Osculosphaera*, for hyaline spheroidal vesicle with a circular rimmed opening.  
256 However this genus has rigid walls, with radial fractures in compression and  
257 tridimensional shape in chert, that is not observed in our material where the  
258 specimens are flattened and folded in compressions, evidencing flexible walls (Pl. 2f).  
259 Porter and Riedman (2016) synonymized some specimens of *L. kulgunica* with  
260 *Kaibabia gemmulella* observed in the 780-740 Ma Chuar Group, US (*Leiosphaeridia*  
261 sp. A in Nagy et al., 2009) but this species has an ornamented operculum. The  
262 absence of an operculum in the specimens of the Atar/El Mreïti Group assemblage  
263 makes difficult the comparison.

264 Leiospheres may also occur as colonies of a few specimens surrounded by a  
265 membrane (Pl. 2l) or large colonies without enveloping membranes, such as  
266 *Synsphaeridium* spp. (Pl. 3r and s; Suppl. Fig. 1B and 3). Other types of coccoidal

267 colonies include four specimens of cf. *Coneosphaera* sp., an association of a single,  
268 ~20-40  $\mu\text{m}$  in diameter, spheroidal vesicle surrounded by few smaller (~5-10  $\mu\text{m}$ )  
269 contiguous vesicles (Pl. 1l); numerous specimens of *Eomicrocystis irregularis*  
270 (irregular cluster of ~2-6  $\mu\text{m}$  small vesicles, Pl. 1m) and *E. malgica* (spheroidal  
271 cluster of ~2-4  $\mu\text{m}$  small vesicles, Pl. 1n), and monostromatic sheets of *Ostiana*  
272 *microcystis*, a colony of closely packed (~10  $\mu\text{m}$  in diameter) vesicles deformed by  
273 mutual compression in a polygonal pattern (Pl. 2s). *Spumosina rubiginosa* (Pl. 3 q) is  
274 a spheroidal aggregate (~40  $\mu\text{m}$  in diameter) of spongy appearance, abundant in  
275 carbonates.

#### 276 **Ornamented acritarchs**

277 The Atar/El Mreïti assemblage also preserves a modest diversity of acritarchs  
278 with walls ornamented with thin granulae, sometimes also bearing a protrusion, thick  
279 verrucae, concentric or perpendicular striations, an equatorial flange, or enclosing  
280 another vesicle. Ornamented sphaeromorphs with thin and granular walls include two  
281 species differing only by their minimum diameter: rare *Leiosphaeridia atava* (Pl. 2a  
282 and b), 70-1000  $\mu\text{m}$  in diameter, and common *L. obsuleta* (Pl. 2i), 10-70  $\mu\text{m}$  in  
283 diameter. *Gemmuloides doncookii* (1 specimen observed, Pl. 1o) also has a  
284 shagreenate wall, but bears one very small spheroidal bud-like protrusion (7.1  $\mu\text{m}$  in  
285 diameter, on a 67.5  $\mu\text{m}$  in diameter vesicle).

286 Rare acritarchs are decorated with an equatorial flange, such as the thin-  
287 walled *Simia annulare* (n=5, ~200  $\mu\text{m}$  in diameter, Pl. 3e). The assemblage also  
288 includes disphaeromorphs such as the common *Pterospermopsimorpha insolita*, a  
289 ~20  $\mu\text{m}$  in diameter smooth-walled vesicle in a ~40  $\mu\text{m}$  in diameter smooth-walled

290 envelope (Pl. 3b and c), and rare *P. pileiformis*, a ~40 µm in diameter vesicle in a ~90  
291 µm in diameter shagreenate envelope (Pl. 3d).

292 *Spiromorpha segmentata* (Pl. 3o and p) is an ovoidal vesicle with closed  
293 rounded ends (65.0-122.5 µm in length and 38.8-57.5 µm in width, n=3). The vesicle  
294 surface shows about 1 µm parallel grooves delimiting stripes (n = 10 to 13 per  
295 specimen) with uneven spacing (3.8-12.1 µm), distributed perpendicular to the main  
296 body axis. The grooves are a surface feature and there are no septae within the  
297 vesicle. *Valeria lophostriata* is also ornamented by striations but the vesicle is  
298 spheroidal and the striations are regularly spaced, thin, and distributed concentrically  
299 (Pl. 4j and k). Only one specimen was observed.

300 Another distinctive but rare species in the assemblage is *Vidaloppala* sp., a  
301 ~50 µm in diameter ovoidal vesicle showing a wall surface ornamented by 1.78 to  
302 2.83 µm bulbous verrucae (Pl. 4l). It differs from *V. verrucata* recently revised in  
303 Riedman and Porter (2016) by the larger size of the verrucae (~1 µm in diameter; 1  
304 to 1.5 µm in the type material originally described by Vidal, 1981, and Vidal and  
305 Siedlecka, 1983, as *Kildinosphaera verrucata*). The diagnosis is not emended here  
306 because only one specimen of *Vidaloppala* was observed. The wall ornamentation of  
307 this specimen shows ovoidal solid verrucae, and clearly differs from some specimens  
308 of *T. aimika* which have a higher vesicle diameter, a thinner and more translucent  
309 wall, and bear small conical or tubular and hollow processes.

### 310 **Process-bearing (acanthomorph) acritarchs**

311 Three species of process-bearing acritarchs are preserved in the Atar/EI Mreiti  
312 Group. Two specimens of *Comasphaeridium tonium* occur in a single horizon of the  
313 Khatt Formation, at the base of the stratigraphy. This species consists of 37.5 µm in



314 diameter vesicles, densely covered with numerous, 2-6  $\mu\text{m}$  long and  $< 0.5 \mu\text{m}$  thin  
315 hair-like, simple (unbranched) and flexible processes that are regularly distributed  
316 around the vesicle (Pl. 1i-k). The Taoudeni specimens are only slightly smaller than  
317 those reported in the Neoproterozoic Alinya Formation, Australia (Zang, 1995;  
318 Riedman and Porter, 2016) ranging from 40-58  $\mu\text{m}$  in diameter, thus probably falls  
319 within the range of the morphological variability of this species. The generic  
320 assignment in Zang (1995) is considered dubious due to the broad diagnosis of this  
321 originally Mesozoic genus (Riedman and Porter, 2016), but the material preserved  
322 here is too limited to propose a revision.

323 The Taoudeni assemblage also includes large populations of the distinctive  
324 species *Trachyhystrichosphaera aimika*, a characteristic acanthomorph acritarch with  
325 a widely variable morphology (Butterfield et al, 1994). This species occurs as ovoidal  
326 vesicles (100.6-275  $\mu\text{m}$  in diameter, mean = 168.4  $\mu\text{m}$ , SD = 45,2  $\mu\text{m}$ , n = 16)  
327 bearing one to numerous, irregularly distributed heteromorphic hollow cylindrical  
328 and/or conical processes, 1.7 to 12.5  $\mu\text{m}$  in width and 4.0 to 25.0  $\mu\text{m}$  in length, and  
329 communicating with the vesicle interior (Pl.3 v, Pl. 4a-e). The cylindrical or conical  
330 processes can be broken at the end or folded in compression on the wall surface  
331 revealing the hollow diagnostic feature of the processes. *T. aimika* is abundant close  
332 to the base of the stratigraphy, in calcareous green-grey shales of the En Nesoar  
333 Formation (n=184), and rare in the Khatt Formation (n=1) (Suppl.Fig 1B). One  
334 specimen was observed in the S4 core in the time correlative Unit I-5 of the Aguel el  
335 Mabha Formation. A single specimen of *T. botula* (400  $\mu\text{m}$  in length, 190-160  $\mu\text{m}$  in  
336 width, Pl. 4f-i), a species similar to *T. aimika* but differing in the length/width ratio ( $>2$ )  
337 (Tang et al., 2003) was observed in the En Nesoar Formation.

338 **Filamentous microfossils**



339 A variety of filamentous microfossils are identified throughout the Atar/EI Mreïti  
340 Group, ranging from simple straight or spiraled smooth-walled filamentous sheaths,  
341 striated sheaths, bundles of filaments, elongate vesicles, to filamentous colonies with  
342 or without envelope, and multicellular microfossils. They are briefly described below.

343 Eight species of *Siphonophycus* are distinguished in the assemblage on the  
344 basis of cross-sectional diameter (revision in Butterfield et al., 1994): *S. thulenema*:  
345 0.5  $\mu\text{m}$ ; *S. septatum*: 1-2  $\mu\text{m}$ ; *S. robustum*: 2-4  $\mu\text{m}$ ; *S. typicum*: 4-8  $\mu\text{m}$ ; *S. kestron*: 8-  
346 16  $\mu\text{m}$ ; and *S. solidum*: 16-32  $\mu\text{m}$ ; and two additional larger species including *S.*  
347 *punctatum* (Maithy, 1975): 32-64  $\mu\text{m}$  and *S. gigas* (Tang et al., 2013): 64-128  $\mu\text{m}$   
348 (Table 1, Pl. 3f-n). *Obruchevella* spp. are also unbranched aseptate filamentous  
349 microfossils, but they differ by their helically coiled morphology (Pl. 2q and r). The  
350 filamentous diameter and the helix diameter are usually uniform in a single specimen  
351 but highly variable from one to the other. Two species of striated sheaths of the  
352 genus *Tortunema* are distinguished by their diameter: *T. patomica*, 25-60  $\mu\text{m}$  in  
353 diameter (Pl. 3u) and *T. wernadskii*, 10-25  $\mu\text{m}$  in diameter (Pl. 3t). The surface  
354 features (spacing between annulations) is an unreliable taxonomic character of  
355 *Tortunema* species as it could change through the filament (Butterfield et al., 1994).  
356 Bundles of parallel, very thin, ~1.5-2.5  $\mu\text{m}$  in diameter, nonseptate filamentous  
357 sheaths are identified as *Polytrichoides lineatus* (Pl. 3a). *Pellicularia tenera* (Pl. 2t) is  
358 a ribbon-like flexible sheath, with longitudinal folds.

359 Two species of *Navifusa*, relatively large single elongate vesicles, are present  
360 in the Taoudeni assemblage (following taxonomic revision by Hofmann and  
361 Jackson, 1994): *N. actinomorpha* with a tapered end (1 specimen, Pl. 2m) and *N.*  
362 *majensis* with a smaller size and ovoid shape (several specimens, Pl. 2n).

363 *Arctacellularia tetragonalis* was previously reported in the Taoudeni  
364 assemblage (Lottorali et al., 2009), and abundant specimens were observed in the  
365 present study. It includes one to several barrel to ovoidal vesicles attached in chain,  
366 and characterized by lanceolate folds or lens-shaped thickenings in the contact area  
367 between adjacent cells (Pl. 1 a-d). The different species of this genus have been  
368 recently synonymized following a revision by Baludikay et al (2016). Other  
369 filamentous colonies of packed spheroidal cells without external sheath include two  
370 species of the genus *Chlorogloeaopsis*: *C. contexta* has indistinct rows of cells and  
371 cell diameter ranging from 1 to 5  $\mu\text{m}$ , and *C. kanshiensis* has 2 or 3 distinct rows of  
372 cells, 10–15  $\mu\text{m}$  in diameter (revision in Hofmann and Jackson, 1994; Baludikay et al,  
373 2016).

374 *Polysphaeroides* sp. (Pl. 2u) is another type of filamentous colony of small 7.0-  
375 11.0  $\mu\text{m}$  in diameter spheroidal cells, enclosed in a 30.0  $\mu\text{m}$  in width and 95.0  $\mu\text{m}$  in  
376 length sheath with broken ends. The cells have dark-brown or black opaque internal  
377 inclusions, are not in close contact and are distributed in approximately two  
378 alternating lines, in a staggered pattern. Both filamentous sheath and spheroids show  
379 folds and are light-grey to light-brown in color. *Polysphaeroides* sp. differs from *P.*  
380 *filiformis* (sheath closed at both ends) by the distribution of internal spheroids which  
381 are not aggregated in pairs, tetrads or octads, nor in close contact but clearly isolated  
382 (Vorob'eva et al., 2009, 2015). It also differs from *P. nuclearis* by the slightly larger  
383 size and irregular distribution of the internal spheroids (Jankauskas et al., 1989).  
384 Populations of *P. filiformis* from the Mbuyi-Mayi Supergroup, DRC have comparable  
385 dimensions of internal cells and sheaths (see revision by Baludikay et al., 2016), but  
386 the internal spheroids are arranged into three different ways in the sheath: 1 or 3  
387 rows of cells; multiples colonies of tiny cells as well as cells overlapping each other

388 with a random distribution. To our knowledge, filamentous microfossils showing the  
389 morphological features observed here (staggered pattern and isolated individual  
390 cells) have not yet been reported in the literature, however only one specimen was  
391 observed preventing the definition of a new species at this point.

392 The more complex filamentous microfossils of the Taoudeni assemblage occur  
393 as five morphotypes of the multicellular microfossil *Jacutianema solubila* described  
394 by Butterfield (2004) occur in the Taoudeni assemblage (Pl. 1p-u), including: (1)  
395 isolated 'simple' botuliform vesicle, ellipsoidal or cylindroidal, non-septate with  
396 rounded ends and sometimes with an inner darker elongate organic axial inclusion  
397 (Pl. 1p and q), (2) chain-like aggregates of at least two botuliform vesicles, and  
398 occasionally showing a incomplete constriction on one side (Pl.1r), (3) similar  
399 morphotype to (2) with one laterally associated thin-walled vesicle (Pl.1s), (4)  
400 spheroidal vesicle communicating with a large filamentous extension connected,  
401 sometimes with organic axial inclusion (Pl.1t), and (5) incompletely divided thick-  
402 walled vesicle showing lateral constrictions (presumed Gongrosira-phase described  
403 in Butterfield 2004; Pl.1, u).

404 In addition to the species described above, two other entities, unreported  
405 elsewhere at our knowledge, were observed and called unnamed forms A and B. The  
406 unnamed form A (Pl. 4m and n) is a ~4.5-5.0  $\mu\text{m}$  wide flat ribbon or flattened sheath  
407 (it is not clear if this is hollow or not), yellow in color, with an echinate or granular  
408 surface (as evidenced by tiny ~1-2  $\mu\text{m}$  pointed spines). Only one specimen is  
409 observed in the Khatt Formation, S2 core. The unnamed form B (Pl. 4o and p) is a  
410 fragment of a relatively large filamentous sheath (22.5  $\mu\text{m}$  in width and 205  $\mu\text{m}$  in  
411 length) with a thin verrucate surface (verrucae of 1.4 to 2.1  $\mu\text{m}$  in diameter). The

412 filament is brown with slightly darker-brown verrucae. Two specimens are observed  
413 in the Khatt Formation in the S2 core.

414 Abundant fragment of benthic microbial mats are observed in black shales of  
415 the En Nesoar and Tourist formations (S2 core). They consist on large amorphous  
416 organic sheets with numerous embedded pyritized filaments (Pl. 2o and p),  
417 previously identified as *Nostocomorpha* sp. by Hofmann and Jackson (1994).

## 418 7. Biological affinities of the Atar/EI Mreïti Group assemblage

419 Among the 48 distinct entities recognized within the Atar/EI Mreïti assemblage  
420 (Table 1), we believe that 11 species can be classified with confidence as  
421 eukaryotes, including four distinct populations of acritarchs ornamented with an  
422 equatorial flange (*Simia annulare*), or transverse striations (*Spiromorpha*  
423 *segmentata*), concentric striations (*Valeria lophostriata*), and verrucae (*Vidaloppala*  
424 sp.); three populations of smooth-walled sphaeromorphs with: a circular opening  
425 interpreted as a sophisticated excystment structure - a pylome - (*Leiosphaeridia*  
426 *kulgunica*), or enclosing another vesicle (*Pterospermopsimorpha insolita* and *P.*  
427 *pileiformis*); one population of multicellular botuliform vesicles (*Jacutianema solubila*),  
428 and three process-bearing (acanthomorphic) acritarchs (*Comasphaeridium tonium*,  
429 *Trachyhystrichosphaera aimika* and *T. botula*). These species are considered as  
430 unambiguous eukaryotes because they combine two or more of the following  
431 characters unknown in extant prokaryotes (Javaux et al., 2003, 2004; Knoll et al,  
432 2006). These characters may include the presence of a complex wall structure and a  
433 surface ornamentation, the presence of processes extending from the vesicle wall,  
434 the presence of an excystment structure, combined with a large diameter and a  
435 recalcitrant kerogenous wall (resistant to acid-maceration). Size is not a criteria in

436 itself since 1-2  $\mu\text{m}$  picoeukaryotes and large Bacteria do exist in nature. Additional  
437 criteria, untested here, may also include a complex wall ultrastructure and a wall  
438 chemistry unique to extant eukaryotes: protists (Javaux et al., 2003, 2004; Marshall  
439 et al., 2005).

440 *Trachyhystrichosphaera aimika* has a very plastic morphology suggesting it may  
441 represent metabolically active vegetative cells (Butterfield et al, 1994), and its  
442 complex cellular morphology evidences the evolution of a cytoskeleton, much alike  
443 the older acanthomorph *Tappania plana* (Javaux et al., 2001; Javaux and Knoll, in  
444 press). Also similarly to recent suggestions for *Tappania* (Javaux and Knoll, in press),  
445 *Trachyhystrichosphaera* also could also be osmotrophic, using its processes to  
446 increase the surface area for absorption. Similar functional arguments had been  
447 proposed for the Neoproterozoic Shaler Group '*Tappania*' sp. by Butterfield (2005,  
448 2015) who compared it first to a fungus.

449 For the vast remaining majority (37 entities), the morphology is simple and they  
450 do not preserve enough taxonomically informative characters to place them with  
451 confidence within prokaryotes or eukaryotes. Among those taxonomically unresolved  
452 species, nine taxa are considered possible eukaryotes and include six smooth-walled  
453 sphaeromorphs (*Chuarina circularis*, *Leiosphaeridia crassa*, *L. jacutica*, *L. minutissima*,  
454 *L. tenuissima*, and *L. ternata*), two sphaeromorph populations with a granular wall  
455 texture (*L. atava*, *L. obsuleta*), and one budding sphaeromorph (*Gemmuloidea*  
456 *doncookii*). However, their biological affinities remains to be tested with further  
457 investigations of their wall ultrastructure and chemistry, using Raman and FTIR  
458 microspectroscopy, and Transmission Electron Microscopy.

459 Six taxa of filamentous microfossils (six species of *Siphonophycus*) are  
460 interpreted as probable prokaryotes, based on their worldwide occurrence mostly in  
461 shallow-water photic zones and frequent associations with silicified stromatolites  
462 (Butterfield et al., 1994; Javaux and Knoll, in press).

463 The remaining distinctive populations cannot be classified even at the level of  
464 domain at this point, and could be prokaryotic or eukaryotic. This group includes  
465 thirteen filamentous taxa (*Arctacellularia tetragonala*, *Navifusa actinomorpha* and *N.*  
466 *majensis*, *Obruchevella* spp., *Pellicularia tenera*, *Polysphaeroides* sp., *Polytrichoides*  
467 *lineatus*, 2 larger species of *Siphonophycus*: *S. gigas* and *S. punctatum*, *Tortunema*  
468 *patomica* and *T. wernadskii* and the two unnamed forms A and B) and nine colonial  
469 forms (*Chlorogloeaopsis contexta*, *C. kanshiensis*, and *C. zairensis*, cf.  
470 *Coneosphaera* sp., *Eomicrocystis irregularis*, *E. malgica*, *Ostiana microcystis*,  
471 *Spumosina rubiginosa* and *Synsphaeridium* spp.). Filaments assigned to  
472 *Obruchevella* are generally interpreted as remains of *Spirulina*-like cyanobacteria,  
473 however other bacteria and some eukaryotic algae show similar spiraling morphology  
474 (Graham et al., 2009; Baludikay et al, 2016).

475 The morphological features observed in the Taoudeni microfossils interpreted as  
476 unambiguous eukaryotes have been reported previously in other contemporaneous  
477 assemblages and their significance as evidence for biological innovations discussed  
478 in details (e.g. Butterfield, 2004; 2015; Javaux et al., 2003; Javaux, 2011; Javaux and  
479 Knoll, in press; Knoll et al., 2006; Knoll, 2015; Riedman and Porter, 2016; Porter and  
480 Riedman, 2016; Tang et al., 2013; Yin et al., 2005).

481 One particular feature, the occurrence of a pylome, a sophisticated excystment  
482 structure, deserves some more discussion here, because of its rare occurrence in

483 mid-Proterozoic successions and importance as biological innovation. Excystment  
484 structures are biologically programmed cyst openings (see discussion in Javaux et  
485 al., 2003; Moczyłowska, 2010). The earliest record of excystment structures show  
486 vesicle opening by medial split in Palaeoproterozoic leiospheres (Zhang 1986; Lamb  
487 et al, 2009) but their eukaryotic or prokaryotic affinities is ambiguous because of  
488 similar openings in a few large pleurocapsalean cyanobacteria envelopes liberating  
489 baeocytes (Waterbury and Stanier, 1978; Javaux, 2011). Medial splits are reported  
490 through the rock record, and in the Taoudeni Basin also (this study, Pl. 2d and h;  
491 Lottaroli et al., 2009). Co-occurrence of medial splits and of an ornamented wall-  
492 surface (e.g. *Valeria lophostriata*) were found in the 1.75-1.4 Ga Ruyang Group,  
493 China (Pang et al., 2015) and in the 1.65 Ga Mallapunyah Formation, Australia  
494 (Javaux et al., 2004), and more complex opening structure at the end of a neck-like  
495 process (e.g. *Tappania plana*) were found in the Roper Group at around 1.5-1.4 Ga  
496 (Javaux et al., 2001; 2003, 2004; Javaux and Knoll, in press).

497 Here, we report the occurrence of *L. kulgunica*, a smooth-walled acritarch (Pl. 2f)  
498 showing a circular opening interpreted as a sophisticated excystment structure  
499 (pylome) requiring more complex biological control than medial split. Unambiguous  
500 pylome structures from *L. kulgunica* were first reported from Russia, in the ca. 1000  
501 Ma Zil'merdak Formation and ca. 925 Ma Podinzer Formation (Jankauskas, 1980;  
502 Jankauskas et al., 1989; Stanevich et al., 2012) and are reported here for the first  
503 time in the 1.1 Ga Atar/El Mreïti Group, slightly extending the stratigraphic range of  
504 this species. Yin et al. (2005) reported possible excystment structures via a circular  
505 opening in some specimens of *Dictyosphaera* and *Shuiyousphaeridium* from the  
506 1.75-1.4 Ga Ruyang Group, China, although some of these could be ripping  
507 structures rather than true pylome structures, but were confirmed by Agić et al.



508 (2015) who reported medial split or occasionally pylome for *Dictyosphaera*  
509 *macroreticulata*, and excystment by medial split or partial rupture for  
510 *Shuiyousphaeridium macroreticulatum*. However the occurrence of different  
511 excystment opening –pylome and medial split–within a single species is intriguing. Liu  
512 et al. (2014) reported the presence of *Osculosphaera hyalina*, a species of psilate  
513 spheroidal vesicle showing an oral collar projecting outward around a well-defined  
514 circular opening (*osculum*), in the  $636.4 \pm 4.9$  to  $551.1 \pm 0.7$  Ma Doushantuo  
515 Formation, China. This species was first described in the  $\sim 820$  Ma ( $<811.5$ - $788$  Ma)  
516 Svanbergfjellet Formation (Butterfield et al., 1994), and also reported in the 850-750  
517 Ma Wynniatt Formation with other unnamed species with circular openings  
518 (Butterfield and Rainbird, 1998), the  $1025 \pm 40$  Ma Lakhanda Group and coeval  
519 strata (see Nagovitsin, 2009), and in the ( $\sim 1.5$ - $1.0$  Ga) Vedreshe and Dzhelindukon  
520 formations, Kamo Group, Russia (Nagovitsin, 2009). As noted above, *L. kulgunica*  
521 seems to differ from *O. kulgunica* proposed by Butterfield et al (2004, p. 43). Peat et  
522 al. (1978) reported possible circular excystment structures in specimens from the  
523 McMinn Formation, 1.5-1.4 Ga Roper Group in northern Australia but this was not  
524 observed by Javaux and Knoll (in press) and a taphonomic origin has been  
525 suggested instead (Schopf and Klein, 1992). Vidal (1976) reported spheroidal  
526 vesicles from the 840-800 Ma Visingsö Group, and Vidal and Ford (1985), from the  
527 780-740 Ma Chuar Group (*Trachysphaeridium laufeldi* and *Leiosphaeridia* sp. A.,  
528 respectively), showing an operculated excystment opening, with conical processes,  
529 or tightly arranged circular granulae respectively. Nagy et al. (2009) reported also  
530 *Leiosphaeridia* sp. A in the 780-740 Ma Chuar Group, renamed *Kaibabia gemmulella*  
531 (Porter and Riedman, 2016) and synonymized with some specimens of *L. kulgunica*  
532 (e.g. Jankauskas, 1980; Jankauskas et al., 1989). As noted above, Porter and



533 Riedman (2016) suggested *K. gemmulella* may be conspecific with *L. kulgunica* but  
534 the absence of an operculum in some specimens of the latter and in the Atar/EI Mreïti  
535 Group assemblage makes difficult the assessment. Regardless of taxonomy, the  
536 report of a pylome in some younger than 1.1 Ga Taoudeni specimens (Aguelt el  
537 Mabha Formation) confirm the evolution of the pylome in mid-Proterozoic  
538 successions worldwide, reported previously in other assemblages from the late  
539 Mesoproterozoic of Russia and Siberia, and Neoproterozoic of Sweden, the US and  
540 China.

## 541 **8. Biostratigraphic and palaeogeographic significance of the Atar/EI Mreïti** 542 **Group microfossil assemblage**

543 Among the taxa present in the Atar/EI Mreïti Group assemblage, many are  
544 common in Proterozoic successions, besides the ubiquitous *Leiosphaeridia* spp. and  
545 *Siphonophycus* spp. Based on summaries in Jankauskas et al. (1989), Sergeev and  
546 Schopf (2010) and a review of the contemporaneous assemblages, Baludikay et al.  
547 (2016) proposed an assemblage characteristic of the middle Mesoproterozoic-early  
548 Neoproterozoic (Tonian), including *Archaeoellipsoides* spp., *Arctacellularia*  
549 *tetragonala* (other species of this genus were synonymized), *Germinosphaera*  
550 *bispinosa*, *Jacutianema solubila*, *Lophosphaeridium granulatum*,  
551 *Trachyhystriosphera aimika*, and *Valeria lophostriata* which are widespread;  
552 *Vidaloppala verrucata* and *Simia annulare* which are common but not ubiquitous, and  
553 *Squamosphaera colonialica* and *Valeria elongata* which have a more restricted  
554 distribution. *T. botula* was reported only in Tonian (Tang et al., 2003; Baludikay et al.,  
555 2016). This assemblage differs from older ones that include the characteristic species  
556 *Tappania plana*, *Dictyosphaera delicata*, *Satka favosa*, *Valeria lophostriata* and less  
557 common *Shuiyousphaeridium macroreticulatum* and *Lineaforma elongata* (Javaux

558 and Knoll, in press), and *Spiromorpha segmentata* (Yin et al., 2005); and younger  
559 pre-Ediacaran assemblages that includes distinctive taxa such as *Cerebrosphaera*  
560 *buickii* and VSMs.

561 Among the middle Mesoproterozoic-early Neoproterozoic species, five species are  
562 present in the Atar/El Mreïti Group assemblage: *A. tetragonala*, *J. solubila*, *S.*  
563 *annulare*, *T. aimika* and *V. lophostriata* confirming a possible middle  
564 Mesoproterozoic–early Neoproterozoic (Tonian) age for the Taoudeni Basin. Only  
565 one specimen of *T. botula* (Pl. 4f-i) is observed in the Atar/El Mreïti Group, extending  
566 the stratigraphic range of this species previously only reported from Tonian rocks  
567 (Tang et al., 2013; Baludikay et al., 2016). A species close to *V. verrucata* (formerly  
568 placed in the invalid genus name *Kildinosphaera* and recently revised in Riedman  
569 and Porter, 2016), *Vidaloppala* sp. (Pl. 4l), is observed in the Atar/El Mreïti Group  
570 assemblage. However, this species differs from *V. verrucata* by the size of the  
571 verrucae, and in the future, detailed measurements of this species in other  
572 assemblages could lead to an emendation of the type species. A specimen of  
573 *Synsphaeridium* (Pl. 3r) could be alternatively identified as *Squamosphaera*  
574 *colonialica* (Tang et al., 2015; Porter and Riedman, 2016), but the diagnostic feature  
575 of domical protrusions freely communicating with the single vesicle interior is not  
576 clearly obvious under the light microscope for this single translucent light-yellow  
577 specimen.

578 A few acritarch taxa are potentially useful as good index microfossils for the late  
579 Mesoproterozoic-early Neoproterozoic: the acanthomorph *Trachyhystrichosphaera*  
580 *aimika* is a good candidate, because it displays distinctive morphologies and is easily  
581 identified despite its large morphological variability, and has a relatively restricted

582 stratigraphic range (when comparing with other mid-Proterozoic taxa) and a large  
583 geographic distribution.

584 Butterfield et al. (1994), Knoll (1996), Tang et al. (2013) and Baludikay et al.  
585 (2016) reported *Trachyhystrichosphaera aimika* as a potential late Mesoproterozoic-  
586 early Neoproterozoic (Tonian) index fossil. Here, we report a new occurrence and  
587 one of the oldest records of *T. aimika* in chronostratigraphically well-constrained  
588 formations of the 1.1 Ga Atar/El Mreïti Group, Taoudeni Basin, Mauritania. At least  
589 174 unambiguous specimens of *T. aimika* have been identified with confidence in the  
590 En Nesoar Formation and are thus constrained by Re/Os datings (Rooney et al.,  
591 2010) on black shales in the S2 core between the  $1107 \pm 12$  Ma overlying Tourist  
592 Formation (139.45 to 143.82 m depth) and the  $1109 \pm 22$  Ma En Nesoar Formation  
593 (206.70 to 207.60 m depth). Moreover, one unambiguous specimen of *T. aimika* was  
594 also observed in the Unit I-5 in the S4 core, correlative of the Aguelte el Mabha  
595 Formation (Fig. 2). Couëffé and Vecoli (2011) reported a putative  
596 *Trachyhystrichosphaera* sp. in the ~1.1-1.0 Ga Volta Basin but the available  
597 illustration of one specimen is ambiguous and no processes are visible. *T. aimika* is  
598 also reported in the  $1025 \pm 40$  Ma Lakhanda Group, Uchur-Maja region, southeastern  
599 Siberia, Russia (Timofeev et al., 1976; Hermann, 1990; Jankauskas et al., 1989;  
600 Semikhatov et al., 2015 for datings); the ~1000-800 Ma Mirojedikha Formation,  
601 Siberia and Urals, Russia (Herman, 1990; Veis et al., 1998); the Neoproterozoic  
602 (<1.05 Ga, detrital zircon age) G-52 drillcore of the Franklin Mountains, northwestern  
603 Canada (Samuelsson and Butterfield, 2001); the ~820 Ma (<811.5-788 Ma, and  
604  $\delta^{13}\text{C}_{\text{carb}}$  chemostratigraphy) Svanbergfjellet Formation, Akademikerbreen Group,  
605 northeastern Spitsbergen, Norway (Butterfield et al., 1994); the ~1100-850 Ma Mbuji-  
606 Mayi Supergroup, RDC (Baludikay et al., 2016); and the 800-700 Ma Draken

607 Conglomerate Formation, northeastern Spitsbergen (Knoll et al., 1991). Note that *T.*  
608 *vidalii* was initially reported in the Mirojedikha Formation (Hermann, 1990) and the  
609 Draken Conglomerate Formation (Knoll et al., 1991) but was later synonymized with  
610 *T. aimika* (Butterfield et al., 1994). The acanthomorph *T. botula*, reported here, also  
611 occurs in the Neoproterozoic Liulaobei Formation (~1000-811 Ma), Huainan Group,  
612 North China (Tang et al., 2013) and the ~1100-850 Ma Mbuji-Mayi Supergroup, RDC  
613 (Baludikay et al., 2016). The new reports of *T. aimika* in western Africa (this study)  
614 and in central Africa (Baludikay et al., 2016) confirm the worldwide palaeogeographic  
615 extension of this taxon in late Mesoproterozoic-early Neoproterozoic marine basins  
616 and its biostratigraphic significance. However, *T. aimika* is not reported in the  
617 contemporaneous (1092 ± 59 Ma) Bylot Supergroup of Canada (Hofmann and  
618 Jackson, 1994; age in Turner and Kamber, 2012) but occurs elsewhere in younger  
619 (Tonian) Wynniatt Fm., Victoria Island, NWT Canada (Butterfield and Rainbird, 1998),  
620 nor in the Tonian of Australia (Cotter, 1999; Hill et al., 2000; Grey et al., 2005;  
621 Riedman and Porter, 2016). *T. aimika* is preferentially preserved (more abundant) in  
622 fluvio-deltaic and marginal shallow-marine facies in Western Africa (abundant in the  
623 En Nesoar Fm., El Mreïti Group, Mauritania, this study); in tidal flats or lagoonal  
624 settings (Draken conglomerate, Knoll et al., 1991), in shallow-water to intertidal  
625 settings in Canada (the Franklin Mountains, level G-52, Samuelsson and Butterfield,  
626 2001), in thin shale beds deposited in shallow subtidal to intertidal settings between  
627 stromatolitic carbonates in Central Africa (Mbuji-Mayi Supergroup, DRC, Baludikay et  
628 al., 2016), in Spitsbergen (Svanbergfjellet Fm., rich levels in the “algal dolomite  
629 member”, Butterfield et al., 1994), in Canada (Wynniatt Fm., Victoria Island, NWT,  
630 Butterfield and Rainbird, 1998; Thomson et al., 2014; and, in China (Tang et al.,  
631 2013). In summary, *T. aimika* is found preferably in intertidal to subtidal facies, but

632 these facies also occur in the Bylot Supergroup and in the Tonian (Supersequence 1  
633 and Alynia Fm., Australia) where this species is not reported. The Bylot Supergroup  
634 might have undergone more restricted conditions in a basin with limited connections  
635 to the global ocean, at least in the Arctic Bay Formation at the base of the  
636 stratigraphy (Turner and Kamber, 2012). Moreover, shale samples were macerated  
637 with standard techniques (Hofmann and Jackson, 1994), so new  
638 micropalaeontological investigations of the promising facies using low manipulation  
639 techniques might reveal more diversity. The studies on Australian material however  
640 have used low agitation maceration techniques on samples from promising shallow-  
641 water facies (Grey et al., 2005; Riedman and Porter, 2016). Differences in  
642 assemblage composition might be due in this case to ecological restrictions of  
643 particular species of eukaryotes linked to redox conditions, nutrient availability, and  
644 palaeogeography, as suggested by similarities in assemblages of prokaryotes but  
645 less for eukaryotes. These hypotheses remain to be tested.

646 *Arctacellularia tetragonala* (recently other species of this genus have been  
647 synonymized to the type species; Baludikay et al., 2016) and *Spiromorpha*  
648 *segmentata* might also have a biostratigraphic potential. This latter species is  
649 common in the Mesoproterozoic Rjuang Group (Yin et al., 2005) but is rarely  
650 observed in the Mesoproterozoic Bahraich Group (Prasad and Asher, 2001).  
651 *Arctacellularia tetragonala* is a distinctive taxon, characterized by the barrel to oval  
652 shape of the single or chain of attached cells and the lanceolate folds at both ends,  
653 but unfortunately has been often confused with other chain-like and sausage shaped  
654 microfossils such as *Jacutianema*, *Archaeoellipsoides*, and *Navifusa* which do not  
655 have the characteristic terminal lens-shaped folds. It is reported as such in the 1092  
656  $\pm$  59 Ma Bylot Supergroup, Baffin Island, Canada (Hofmann and Jackson, 1994); in

657 the Sarda (~1.35-1.25 Ga) and Avadh (ca 1.2-1.15 Ga) formations, Bahraich Group,  
658 Ganga Supergroup, of the Ganga Basin, in India (Prasad and Asher, 2001); in the  
659 1.1 Ga Atar/El Mreïti Group, Mauritania (this study); ~1.1-0.85 Ga, Mbuji-Mayi  
660 (Bushimay) Supergroup, Democratic Republic of Congo (Baludikay et al., 2016); the  
661 ~1000-800 Ma, Mirojedikha Formation, Russia (Jankauskas et al., 1989; Hermann,  
662 1990). Only three specimens of *Spiromorpha segmentata* are present in the Atar/El  
663 Mreïti Group assemblage. However this species also has a distinctive morphology  
664 and restricted stratigraphic distribution, and seems to be restricted to the late  
665 Palaeoproterozoic and Mesoproterozoic, occurring in the present assemblage from  
666 the 1.1 Ga Atar/El Mreïti Group, in the Palaeoproterozoic/Mesoproterozoic Ruyang  
667 Group (1750-1400 Ma, see Lan et al., 2014 and Hu et al., 2014 for datings) in China  
668 (Yin et al. 2005) in addition to *Spiromorpha* sp. (Pang et al., 2015), possibly in the  
669 Yurubchen ( $1499 \pm 43$  to  $1060 \pm 20$  Ma) and Dzhelindukon (1526-1275 Ma to 1265-  
670 1105 Ma) formations, Kamo Group, Central Angara Basin, Siberian Craton where it  
671 was reported as lenticular and medial arcuate cells (Nagovitsin, 2009; fig. 5h and i),  
672 and also in the ~1.25-1.15 Ga, Avadh Fm. and ~1.35-1.25 Ga Sarda Fm., India  
673 where it was reported as *Navifusa segmentatus* (Prasad and Asher, 2001). Further  
674 studies of new assemblages might confirm the global biostratigraphic value of this  
675 species.

676 The overlapping stratigraphic range of *A. tetragonala*, *S. segmentata* and *T.*  
677 *aimika* suggests also a late Mesoproterozoic to early Neoproterozoic age (Tonian) for  
678 the Atar/El Mreïti Group. This age is consistent with Re-Os geochronology (ca. 1.1  
679 Ga, Rooney et al., 2010), chemostratigraphy (~1.2 Ga, Kah et al., 2009) and its  
680 lithostratigraphic occurrence below the Marinoan correlative deposits of the Jbéliat  
681 Group (Álvaro et al., 2007; Shields et al., 2007; Halverson et al., 2007, 2010).

682 The Atar/El Mreïti Group microfossil assemblage with 24 other geological  
683 localities worldwide, ranging from the late Palaeoproterozoic to the late Cryogenian is  
684 summarized in Table 2. (Only the species present in the Atar/El Mreïti Group  
685 assemblage were taken into account and not species present elsewhere but not in  
686 Taoudeni). To confirm the diagnoses, the descriptions and illustrated specimens of  
687 each locality reported in the literature were compared to the published original or  
688 emended diagnosis and illustrations of the type material when available.

689 At least four basins show more similarities when compared to the Atar/El Mreïti  
690 Group assemblage (underlined in bold in Table 2): (1) the ~1100-850 Ma, Mbuji-Mayi  
691 (Bushimay) Supergroup, Democratic Republic of Congo (Baludikay et al., 2016); (2)  
692 the  $1092 \pm 59$  Ma Bylot Supergroup, Baffin Island, Canada (Hofmann and Jackson,  
693 1994); (3) the ~1000-800 Ma, Mirojedikha Formation, Russia (Jankauskas et al.,  
694 1989; Hermann, 1990) and (4) the ~1000-811 Ma, but poorly constrained, Liulaobei  
695 Formation, Huainan region, North China (Tang et al., 2013; Xiao et al., 2014). These  
696 assemblages share more unambiguous eukaryotic species (see Table 1) in common  
697 than with other assemblages, or more total species (without taking into account  
698 *Leiosphaeridia* spp., *Siphonophycus* spp. and *Synpsphaeridium* spp.; which are not  
699 always identified at species level in the literature but are broadly ubiquitous). The Bylot  
700 Supergroup is more similar regarding the prokaryotic species. However, assemblage  
701 differences between the four basins mentioned above and other basins could be  
702 related not only to stratigraphy and palaeogeography but also to ecology and  
703 preservation (depositional facies). However, most assemblages are preserved in  
704 intertidal to subtidal environments, and most basins show redox stratified conditions  
705 but perhaps subtle differences in local basin geometry with restricted connections to  
706 the global ocean and palaeogeography impose ecological restrictions on sensitive



707 species. At this point, it is not possible to estimate the reality of reported differences  
708 and it is probable that careful studies with low manipulation maceration techniques  
709 and more detailed extensive sampling in promising facies and neglected ones will  
710 reveal more diversity and similarities between contemporaneous assemblages.

711 The Mbuji-Mayi Supergroup (Congo) deposited in an intracratonic failed-rift basin  
712 but connected to the ocean, as suggested by its microfossil assemblage. The  
713 deposits of the Mbuji-Mayi Supergroup are recognized as shallow marine and are  
714 divided into the BI Group (mainly siliciclastics) and the BII Group (mostly stromatolitic  
715 carbonates and thinner interbedded shales). During the time period 1000-850 Ma the  
716 Congo-Sao Francisco Craton shifted from between the palaeo-latitude of 30-60°S to  
717 the palaeo-latitude of 30°N (Li et al., 2008). The Bylot Supergroup is a localised rift  
718 graben basin, rather than a setting fully linked to the global ocean (Turner and  
719 Kamber, 2012). At the base of the Bylot Supergroup, the 1092 ± 59 Ma Arctic bay  
720 Fm. deposited under a stratified oxidized-euxinic water mass in an actively  
721 extensional basin (Turner and Kamber, 2012). Microfossils reported by Hofmann and  
722 Jackson (1994) are preserved throughout the Bylot Supergroup, in facies ranging  
723 from intertidal-supratidal to deep basinal palaeoenvironments, but is dominated by  
724 deposition in semi-restricted nearshore, arid to semi-arid environments, north of the  
725 palaeoequator (Hofmann and Jackson, 1994, fig. 9, p.13). According to Hermann  
726 (1990) the Mirojedikha Formation deposited under shallow-water. During the time  
727 period 1000-800 Ma, Siberia was probably located close to the palaeoequator (Li et  
728 al., 2008). The sedimentary basin (Liulaobei Formation) in the Huainan region, China,  
729 may be related to rifting and drifting phases during Rodinia breakup in the early  
730 Neoproterozoic (Tang et al., 2013). During the late Mesoproterozoic (1100-900 Ma),  
731 the North China Bloc was probably located in the tropical periphery, between the



732 palaeoequator and palaeo-latitude of 30°S of the Rodinia supercontinent (Li et al.,  
733 2008; Tang et al., 2013). The West African Craton was also possibly located at the  
734 palaeolatitude of 30°S at 1.1 Ga but then shifted to the palaeo-South pole between  
735 1050-900 Ma (Li et al., 2008). Thus, these geological localities seem to have been all  
736 localized within the inter-tropical zone during their relative time episode of shallow-  
737 water sedimentary deposition, and the presence of ubiquitous species suggest  
738 connections between these basins. However, other palaeogeographic  
739 reconstructions of Rodinia are possible (e.g. Evans, 2013; Johansson et al., 2014).

## 740 9. Conclusions

741 This study reveals a new assemblage of exquisitely preserved organic-walled  
742 microfossils from the largely undersampled African continent. A total of 48 distinct  
743 entities including 11 unambiguous eukaryotes (e.g. ornamented and process-bearing  
744 acritarchs), and 37 taxonomically unresolved taxa (including 9 possible eukaryotes, 6  
745 probable prokaryotes, and 22 other prokaryotic or eukaryotic taxa) were observed in  
746 the Atar/El Mreïti Group assemblage, from the Taoudeni Basin, Mauritania. Locally,  
747 black shales preserve abundant fragments of pyritized benthic microbial mats. This  
748 work improves the diversity previously reported in Proterozoic shales of the Taoudeni  
749 Basin and records a modest diversity of unambiguous eukaryotes for the first time in  
750 the Taoudeni Basin, including one of the oldest records of *T. aimika*, *T. botula* and *L.*  
751 *kulgunica*, the latter documenting an opening through a circular hole interpreted as a  
752 sophisticated excystment structure (pylome) in protists. The assemblage composition  
753 supports a late Meso- to early Neoproterozoic (Tonian) age, in agreement with  
754 previous litho-, chemo- and chronostratigraphic estimations. This study also expands  
755 the palaeogeographic distribution of the Proterozoic biosphere, including early  
756 eukaryotes, 1.1 billion years ago in Western Africa.

757 **Acknowledgements**

758 Research support from BELSPO IAP PLANET TOPERS to J. Beghin (PhD  
759 scholarship) and E. J. Javaux (PI), and ERC Stg ELiTE to J.-Y. Storme (postdoc  
760 fellowship) and E. J. Javaux (PI) are gratefully acknowledged. J.J. Brocks  
761 acknowledges support from the Australian Research Council (DP1095247). We thank  
762 TOTAL S. A. and Jean-Pierre Houzay for access to cores for sampling, M. Giraldo  
763 (ULg) for sample preparation, and three anonymous reviewers for constructive  
764 comments that considerably help to improve the manuscript.

765 **References**

- 766 Agić, H., Moczyłowska, M., Yin, L.-M., 2015. Affinity, life cycle, and intracellular  
767 complexity of organic-walled microfossils from the Mesoproterozoic of Shanxi, China.  
768 *Journal of Paleontology* 89, 28-50.
- 769 Allison, C., Awramik, S., 1989. Organic-walled microfossils from earliest Cambrian or  
770 latest Proterozoic Tindir Group rocks, Northwest Canada. *Precambrian Research* 43,  
771 253-294.
- 772 Álvaro, J.J., Macouin, M., Bauluz, B., Clausen, S., Ader, M., 2007. The Ediacaran  
773 sedimentary architecture and carbonate productivity in the Atar cliffs, Adrar,  
774 Mauritania: Palaeoenvironments, chemostratigraphy and diagenesis. *Precambrian*  
775 *Research* 153, 236-261.
- 776 Amard, B., 1984. Nouveaux éléments de datation de la couverture protérozoïque du  
777 craton ouest-africain : un assemblage de microfossiles (Acritarches) caractéristique  
778 du Riphéen supérieur dans la formation d'Atar (Mauritanie). *C.R. Acad. Sc. Paris*,  
779 *Série II* 299, 1405-1410.

- 780 Amard, B., 1986. Microfossiles (Acritarches) du Protérozoïque supérieur dans les  
781 shales de la formation d'Atar (Mauritanie). *Precambrian Research* 31, 69-95.
- 782 Azmy, K., Kendall, B., Creaser, R.A., Heaman, L., de Oliveira, T.F., 2008. Global  
783 correlation of the Vazante Group, São Francisco Basin, Brazil: Re–Os and U–Pb  
784 radiometric age constraints. *Precambrian Research* 164, 160-172.
- 785 Baludikay, B.K., Storme, J.-Y., François, C., Baudet, D., Javaux, E.J., in review. A  
786 diverse and exquisitely preserved organic-walled microfossil assemblage from the  
787 Meso – Neoproterozoic Mbuji-Mayi Supergroup (Democratic Republic of Congo) and  
788 biostratigraphic constraints. *Precambrian Research*.
- 789 Baludikay, B.K., Storme, J.Y., François, C., Baudet, D., Javaux, E.J., 2016. A diverse  
790 and exquisitely preserved organic-walled microfossil assemblage from the Meso–  
791 Neoproterozoic Mbuji-Mayi Supergroup (Democratic Republic of Congo) and  
792 implications for Proterozoic biostratigraphy. *Precambrian Research* 281, 166-184.
- 793 Bartley, J.K., Kah, L.C., McWilliams, J.L., Stagner, A.F., 2007. Carbon isotope  
794 chemostratigraphy of the Middle Riphean type section (Avzyan Formation, Southern  
795 Urals, Russia): Signal recovery in a fold-and-thrust belt. *Chemical Geology* 237, 211-  
796 232.
- 797 Bartley, J.K., Semikhatov, M.A., Kaufman, A.J., Knoll, A.H., Pope, M.C., Jacobsen,  
798 S.B., 2001. Global events across the Mesoproterozoic–Neoproterozoic boundary: C  
799 and Sr isotopic evidence from Siberia. *Precambrian Research* 111, 165-202.
- 800 BEICIP, 1981. Nouvelles observations géologiques dans le bassin de Taoudeni.  
801 Rapport de la mission de terrain, DMG - DNGM, Paris.

- 802 Benan, C.A.A., Deynoux, M., 1998. Facies analysis and sequence stratigraphy of  
803 Neoproterozoic Platform deposits in Adrar of Mauritania, Taoudeni Basin, West  
804 Africa. *Geol Rundsch* 87, 283-302.
- 805 Bertrand-Sarfati, J., 1972. Paléoécologie de certains stromatolites en récifs des  
806 formations du Précambrien supérieur du groupe d'Atar (Mauritanie, Sahara  
807 occidental): Création d'espèces nouvelles. *Palaeogeography, Palaeoclimatology,*  
808 *Palaeoecology* 11, 33-63.
- 809 Bertrand-Sarfati, J., Moussine-Pouchkine, A., 1985. Evolution and environmental  
810 conditions of Conophyton—Jacutophyton associations in the atar dolomite (upper  
811 Proterozoic, Mauritania). *Precambrian Research* 29, 207-234.
- 812 Bertrand-Sarfati, J., Moussine-Pouchkine, A., 1988. Is cratonic sedimentation  
813 consistent with available models? An example from the Upper Proterozoic of the  
814 West African craton. *Sedimentary Geology* 58, 255-276.
- 815 Bertrand-Sarfati, J., Moussine-Pouchkine, A., 1999. Mauritanian microbial buildups:  
816 meso-neoproterozoic stromatolites and their environment, six days field trip in the  
817 Mauritanian Adrar, Atar, Islamic Republic of Mauritania; guidebook. *Association des*  
818 *Sédimentologues Français* 31, 1-103.
- 819 Blumenberg, M., Thiel, V., Riegel, W., Kah, L.C., Reitner, J., 2012. Biomarkers of  
820 black shales formed by microbial mats, Late Mesoproterozoic (1.1 Ga) Taoudeni  
821 Basin, Mauritania. *Precambrian Research* 196–197, 113-127.
- 822 Butterfield, N.J., 1997. Plankton ecology and the Proterozoic-Phanerozoic transition.  
823 *Paleobiology* 23, 247-262.

- 824 Butterfield, N.J., 2004. A vaucheriacean alga from the middle Neoproterozoic of  
825 Spitsbergen implications for the evolution of Proterozoic eukaryotes and the  
826 Cambrian explosion. *Paleobiology* 30, 231-252.
- 827 Butterfield, N.J., 2005. Probable proterozoic fungi. *Paleobiology* 31, 165-182.
- 828 Butterfield, N.J., 2015. Early evolution of the Eukaryota. *Palaeontology* 58, 5-17.
- 829 Butterfield, N.J., Knoll, A.H., Swett, K., 1994. Paleobiology of the Neoproterozoic  
830 Svanbergfjellet Formation, Spitsbergen. *Lethaia* 27, 76-76.
- 831 Butterfield, N.J., Rainbird, R.H., 1998. Diverse organic-walled fossils, including  
832 "possible dinoflagellates", from the early Neoproterozoic of arctic Canada. *Geology*  
833 26, 963-966.
- 834 Clauer, N., 1976. Chimie isotopique du strontium des milieux sédimentaires.  
835 Application à la géochronologie de la couverture du craton ouest africain. *Mém Sci*  
836 *Géol* 45, 1-256.
- 837 Clauer, N., 1981. Rb—Sr and K—Ar dating of Precambrian clays and glauconies.  
838 *Precambrian Research* 15, 331-352.
- 839 Clauer, N., Caby, R., Jeannette, D., Trompette, R., 1982. Geochronology of  
840 sedimentary and metasedimentary Precambrian rocks of the West African craton.  
841 *Precambrian Research* 18, 53-71.
- 842 Clauer, N., Deynoux, M., 1987. New information on the probable isotopic age of the  
843 late proterozoic glaciation in west africa. *Precambrian Research* 37, 89-94.

- 844 Cotter, K.L., 1999. Microfossils from Neoproterozoic Supersequence 1 of the Officer  
845 Basin, Western Australia. *Alcheringa: An Australasian Journal of Palaeontology* 23,  
846 63-86.
- 847 Couëffé, R., Vecoli, M., 2011. New sedimentological and biostratigraphic data in the  
848 Kwahu Group (Meso- to Neo-Proterozoic), southern margin of the Volta Basin,  
849 Ghana: Stratigraphic constraints and implications on regional lithostratigraphic  
850 correlations. *Precambrian Research* 189, 155-175.
- 851 Deynoux, M., Affaton, P., Trompette, R., Villeneuve, M., 2006. Pan-African tectonic  
852 evolution and glacial events registered in Neoproterozoic to Cambrian cratonic and  
853 foreland basins of West Africa. *Journal of African Earth Sciences* 46, 397-426.
- 854 Evans, D.A.D., 2013. Reconstructing pre-Pangean supercontinents. *Geological*  
855 *Society of America Bulletin* 125, 1735-1751.
- 856 Fairchild, I.J., Marshall, J.D., Bertrand-Sarfati, J., 1990. Stratigraphic shifts in carbon  
857 isotopes from Proterozoic stromatolitic carbonates (Mauritania): influences of primary  
858 mineralogy and diagenesis. *American Journal of Science* 290-A, 46-79.
- 859 François, C., Baludikay, B.K., Storme, J.-Y., Baudet, D., Javaux, E.J., 2015.  
860 Geochronological constraints on the diagenesis of the Mbuji-Mayi Supergroup,  
861 Democratic Republic of Congo (RDC), Goldschmidt
- 862 Frank, T.D., Kah, L.C., Lyons, T.W., 2003. Changes in organic matter production and  
863 accumulation as a mechanism for isotopic evolution in the Mesoproterozoic ocean.  
864 *Geological Magazine* 140, 397-420.

- 865 Gilleaudeau, G.J., Kah, L.C., 2013a. Carbon isotope records in a Mesoproterozoic  
866 epicratonic sea: Carbon cycling in a low-oxygen world. *Precambrian Research* 228,  
867 85-101.
- 868 Gilleaudeau, G.J., Kah, L.C., 2013b. Oceanic molybdenum drawdown by epeiric sea  
869 expansion in the Mesoproterozoic. *Chemical Geology* 356, 21-37.
- 870 Gilleaudeau, G.J., Kah, L.C., 2015. Heterogeneous redox conditions and a shallow  
871 chemocline in the Mesoproterozoic ocean: Evidence from carbon–sulfur–iron  
872 relationships. *Precambrian Research* 257, 94 - 108.
- 873 Golovenok, V.K., Belova, M.Y., 1984. Riphean microbiota in cherts of the Billyakh  
874 Group on the Anabar Uplift. *Paleontol. J.* 4, 20-30.
- 875 Graham, L.E., Graham, J.M., Wilcox, L.W., 2009. *Algae*. Pearson.
- 876 Grey, K., 1999. A modified palynological preparation technique for the extraction of  
877 large Neoproterozoic acanthomorph acritarchs and other acid-insoluble microfossils:  
878 Western Australia Geological Survey, Record 1999/10. 23.
- 879 Grey, K., Hocking, R.M., Stevens, M.K., Bagas, L., Carlsen, G.M., Irimies, F., Pirajno,  
880 F., Haines, P.W., Apak, S.N., 2005. Lithostratigraphic nomenclature of the Officer  
881 Basin and correlative parts of the Paterson Orogen, Western Australia, in: Survey,  
882 W.A.G. (Ed.), Perth, p. 89.
- 883 Gueneli, N., Brocks, J.J., Legendre, E., 2012. 1.1 Billion-years-old biomarkers from a  
884 microbial mat. *Mineralogical Magazine* 76, 1787.

- 885 Gueneli, N., McKenna, A.M., Krajewski, L.C., Che, H., Boreham, C., Ohkouchi, N.,  
886 Poulton, S.W., Beghin, J., Javaux, E.J., Brocks, J.J., 2015. Porphyrins from 1.1 Gyr  
887 Benthic Mats, Goldschmidt, Prague.
- 888 Halverson, G.P., Dudás, F.Ö., Maloof, A.C., Bowring, S.A., 2007. Evolution of the  
889  $^{87}\text{Sr}/^{86}\text{Sr}$  composition of Neoproterozoic seawater. *Palaeogeography,*  
890 *Palaeoclimatology, Palaeoecology* 256, 103-129.
- 891 Halverson, G.P., Hoffman, P.F., Schrag, D.P., Maloof, A.C., Rice, A.H.N., 2005.  
892 Toward a Neoproterozoic composite carbon-isotope record. *Geological Society of*  
893 *America Bulletin* 117, 1181-1207.
- 894 Halverson, G.P., Wade, B.P., Hurtgen, M.T., Barovich, K.M., 2010. Neoproterozoic  
895 chemostratigraphy. *Precambrian Research* 182, 337-350.
- 896 Hermann, T.N., 1990. *Organic world one billion years ago.* Nauka, Leningrad.
- 897 Hermann, T.N., Podkovyrov, V.N., 2010. A Discovery of Riphean Heterotrophs in the  
898 Lakhanda Group of Siberia *Paleontological Journal [English version]* 44, 374-383.
- 899 Hill, A.C., Cotter, K.L., Grey, K., 2000. Mid-Neoproterozoic biostratigraphy and  
900 isotope stratigraphy in Australia. *Precambrian Research* 100, 281-298.
- 901 Hofmann, H.J., Jackson, G.D., 1994. Shale-facies Microfossils from the Proterozoic  
902 Bylot Supergroup, Baffin Island, Canada. *Paleontological Society Memoirs* 37 68, 39.
- 903 Hu, G., Zhao, T., Zhou, Y., 2014. Depositional age, provenance and tectonic setting  
904 of the Proterozoic Ruyang Group, southern margin of the North China Craton.  
905 *Precambrian Research* 246, 296 - 318.



- 906 Ivanovskaya, A.V., Timofeev, B.V., Trompette, R., 1980. New data on the  
907 stratigraphy and lithology of the Upper Precambrian of the 'Adrar de Mauritanie'  
908 (North-Western Africa) [in Russian], in: Mitrofanov (Ed.), Principles and criteria of  
909 subdivisions of Precambrian in mobile zones. Acad. Sci. USSR, Leningrad, pp. 256-  
910 279.
- 911 Jankauskas, T.V., 1980. Shishenyakskaya mikrobiota verkhnego rifeya Yuzhnogo  
912 Urala [The Upper Riphean Shishenyak microbiota from Southern Urals] Doklady  
913 Akademii SSSR 251, 190-192.
- 914 Jankauskas, T.V., Mikhailova, N.S., Hermann, T.N., 1989. Microfossillii Dokembriya  
915 SSSR [Precambrian microfossils of the USSR]. Akademiya Nauk SSSR, Institut  
916 Geologii i Geokhronologii Dokembriya, Nauka, Leningrad.
- 917 Javaux, E.J., 2011. Early eukaryotes in Precambrian oceans, Origins and Evolution  
918 of Life. An Astrobiological Perspective. Cambridge University Press, pp. 414-449.
- 919 Javaux, E.J., Knoll, A.H., in press. Micropaleontology of the lower Mesoproterozoic  
920 Roper Group, Australia and implications for early eukaryote evolution. Journal of  
921 Paleontology.
- 922 Javaux, E.J., Knoll, A.H., Walter, M., 2003. Recognizing and Interpreting the Fossils  
923 of Early Eukaryotes. Orig Life Evol Biosph 33, 75-94.
- 924 Javaux, E.J., Knoll, A.H., Walter, M.R., 2001. Morphological and ecological  
925 complexity in early eukaryotic ecosystems. Nature 412, 66-69.
- 926 Javaux, E.J., Knoll, A.H., Walter, M.R., 2004. TEM evidence for eukaryotic diversity  
927 in mid-Proterozoic oceans. Geobiology 2, 121-132.

- 928 Johansson, Å., 2014. From Rodinia to Gondwana with the 'SAMBA' model—A distant  
929 view from Baltica towards Amazonia and beyond. *Precambrian Research* 244, 226-  
930 235.
- 931 Kah, L.C., Bartley, J.K., Stagner, A.F., 2009. Reinterpreting a Proterozoic Enigma:  
932 *Conophyton-Jacutophyton* Stromatolites of the Mesoproterozoic Atar Group,  
933 Mauritania, *Perspectives in Carbonate Geology*. John Wiley & Sons, Ltd, pp. 277-  
934 295.
- 935 Kah, L.C., Bartley, J.K., Teal, D.A., 2012. Chemostratigraphy of the Late  
936 Mesoproterozoic Atar Group, Taoudeni Basin, Mauritania: Muted isotopic variability,  
937 facies correlation, and global isotopic trends. *Precambrian Research* 200–203, 82-  
938 103.
- 939 Kah, L.C., Lyons, T.W., Chesley, J.T., 2001. Geochemistry of a 1.2 Ga carbonate-  
940 evaporite succession, northern Baffin and Bylot Islands: implications for  
941 Mesoproterozoic marine evolution. *Precambrian Research* 111, 203-234.
- 942 Kah, L.C., Sherman, A.G., Narbonne, G.M., Knoll, A.H., Kaufman, A.J., 1999.  $\delta^{13}\text{C}$   
943 stratigraphy of the Proterozoic Bylot Supergroup, Baffin Island, Canada: implications  
944 for regional lithostratigraphic correlations. *Canadian Journal of Earth Sciences* 36,  
945 313-332.
- 946 Kaufman, A.J., Knoll, A.H., 1995. Neoproterozoic variations in the C-isotopic  
947 composition of seawater: stratigraphic and biogeochemical implications. *Precambrian*  
948 *Research* 73, 27-49.
- 949 Knoll, A.H., 1984. Microbiotas of the late Precambrian Hunnberg Formation,  
950 Nordaustlandet, Svalbard. *Journal of Paleontology* 58, 131-162.

- 951 Knoll, A.H., 1992. Vendian microfossils in metasedimentary cherts of the Scotia  
952 Group, Prins Karls Forland, Svalbard. *Palaeontology* 35, 751-774.
- 953 Knoll, A.H., 1996. Archean and Proterozoic paleontology, in: Jansonius, J.,  
954 McGregor, D.C. (Eds.), *Palynology: principles and applications*. American  
955 Association of Stratigraphic Palynologists Foundation, pp. 51-80.
- 956 Knoll, A.H., 2000. Learning to tell Neoproterozoic time. *Precambrian Research* 100,  
957 3-20.
- 958 Knoll, A.H., 2014. Paleobiological Perspectives on Early Eukaryotic Evolution. *Cold  
959 Spring Harbor Perspectives in Biology* 6.
- 960 Knoll, A.H., Calder, S., 1983. Microbiotas of the late Precambrian Ryssö Formation,  
961 Nordaustlandet, Svalbard. *Palaeontology* 26, 467-496.
- 962 Knoll, A.H., Javaux, E.J., Hewitt, D., Cohen, P., 2006a. Eukaryotic organisms in  
963 Proterozoic oceans. *Philosophical Transactions of the Royal Society B: Biological  
964 Sciences* 361, 1023-1038.
- 965 Knoll, A.H., Kaufman, A.J., Semikhatov, M.A., 1995. The carbon-isotopic composition  
966 of Proterozoic carbonates: Riphean successions from northwestern Siberia (Anabar  
967 Massif, Turukhansk Uplift). *American Journal of Science* 295, 823-850.
- 968 Knoll, A.H., Swett, K., Mark, J., 1991a. Paleobiology of a Neoproterozoic Tidal  
969 Flat/Lagoonal Complex: The Draken Conglomerate Formation, Spitsbergen. *Journal  
970 of Paleontology* 65, 531-570.

- 971 Knoll, A.H., Swett, K., Mark, J., 1991b. Paleobiology of a Neoproterozoic tidal  
972 flat/lagoonal complex; the Draken conglomerate formation, Spitsbergen. *Journal of*  
973 *Paleontology* 65, 531-570.
- 974 Knoll, A.H., Walter, M., Narbonne, G.U.Y., Christie-Blick, N., 2006b. The Ediacaran  
975 Period: a new addition to the geologic time scale. *Lethaia* 39, 13-30.
- 976 Lahondère, D., Roger, J., Le Métour, J., Donzeau, M., Guillocheau, F., Helm, C.,  
977 Thiéblemont, D., Cocherie, A., Guerrot, C., 2005. Notice explicative des cartes  
978 géologiques à 1/200 000 et 1/500 000 de l'extrême sud de la Mauritanie, Rapport  
979 BRGM/RC-54273-FR. DMG Ministère des Mines et de l'Industrie, Nouakchott, p.  
980 610.
- 981 Lahondère, D., Thiéblemont, D., Goujou, J.-C., Roger, J., Moussine-Pouchkine, A.,  
982 LeMetour, J., Cocherie, A., Guerrot, C., 2003. Notice explicative des cartes  
983 géologiques et gîtologiques à 1/200 000 et 1/500 000 du Nord de la Mauritanie.  
984 Volume 1. DMG, Ministère des Mines et de l'Industrie, Nouakchott.
- 985 Lamb, D.M., Awramik, S.M., Chapman, D.J., Zhu, S., 2009. Evidence for eukaryotic  
986 diversification in the ~1800 million-year-old Changzhougou Formation, North China.  
987 *Precambrian Research* 173, 93-104.
- 988 Lan, Z., Li, X., Chen, Z.-Q., Li, Q., Hofmann, A., Zhang, Y., Zhong, Y., Liu, Y., Tang,  
989 G., Ling, X., Li, J., 2014. Diagenetic xenotime age constraints on the Sanjiaotang  
990 Formation, Luoyu Group, southern margin of the North China Craton: Implications for  
991 regional stratigraphic correlation and early evolution of eukaryotes. *Precambrian*  
992 *Research* 251, 21 - 32.

- 993 Li, Z.X., Bogdanova, S.V., Collins, A.S., Davidson, A., Waele, B.D., Ernst, R.E.,  
994 Fitzsimons, I.C.W., Fuck, R.A., Gladkochub, D.P., Jacobs, J., Karlstrom, K.E., Lu, S.,  
995 Natapov, L.M., Pease, V., Pisarevsky, S.A., Thrane, K., Vernikovskiy, V., 2008.  
996 Assembly, configuration, and break-up history of Rodinia: A synthesis. *Precambrian*  
997 *Research* 160, 179 - 210.
- 998 Liu, P., Xiao, S., Yin, C., Chen, S., Zhou, C., Li, M., 2014. Ediacaran Acanthomorphic  
999 Acritarchs and Other Microfossils From Chert Nodules of the Upper Doushantuo  
1000 Formation In the Yangtze Gorges Area, South China. *Journal of Paleontology* 88, 1-  
1001 139.
- 1002 Lottaroli, F., Craig, J., Thusu, B., 2009. Neoproterozoic-Early Cambrian  
1003 (Infracambrian) hydrocarbon prospectivity of North Africa: a synthesis. *Geological*  
1004 *Society, London, Special Publications* 326, 137-156.
- 1005 Macdonald, F.A., Schmitz, M.D., Crowley, J.L., Roots, C.F., Jones, D.S., Maloof,  
1006 A.C., Strauss, J.V., Cohen, P.A., Johnston, D.T., Schrag, D.P., 2010. Calibrating the  
1007 Cryogenian. *Science* 327, 1241-1243.
- 1008 Maithy, P.K., 1975. Micro-organisms from the Bushimay System (Late Pre-Cambrian)  
1009 of Kanshi, Zaire. *The Palaeobotanist* 22, 133-149.
- 1010 Marshall, C., Javaux, E., Knoll, a., Walter, M., 2005. Combined micro-Fourier  
1011 transform infrared (FTIR) spectroscopy and micro-Raman spectroscopy of  
1012 Proterozoic acritarchs: A new approach to Palaeobiology. *Precambrian Research*  
1013 138, 208-224.

- 1014 Mendelson, C.V., Schopf, J.W., 1982. Proterozoic microfossils from the Sukhaya  
1015 Tunkuska, Shorikha, and Yudoma Formations of the Siberian Platform, USSR.  
1016 *Journal of Paleontology* 56, 42-83.
- 1017 Moczyłowska, M., 2010, Life cycle of early Cambrian microalgae from the Skiagia-  
1018 plexus acritarchs. *Journal of Paleontology* 84, 216–230.
- 1019 Moczyłowska, M., Nagovitsin, K.E., 2012. Ediacaran radiation of organic-walled  
1020 microbiota recorded in the Ura Formation, Patom Uplift, East Siberia. *Precambrian*  
1021 *Research* 198–199, 1-24.
- 1022 Moussine-Pouchkine, A., Bertrand-Sarfati, J., 1997. Tectonosedimentary  
1023 subdivisions in the neoproterozoic to Early Cambrian cover of the taoudenni Basin  
1024 (Algeria-Mauritania-Mali). *Journal of African Earth Sciences* 24, 425-443.
- 1025 Nagovitsin, K., 2009. Tappania-bearing association of the Siberian platform:  
1026 Biodiversity, stratigraphic position and geochronological constraints. *Precambrian*  
1027 *Research* 173, 137-145.
- 1028 Nagovitsin, K.E., Rogov, V.I., Marusin, V.V., Karlova, G.A., Kolesnikov, A.V., Bykova,  
1029 N.V., Grazhdankin, D.V., 2015. Revised Neoproterozoic and Terreneuvian  
1030 stratigraphy of the Lena-Anabar Basin and north-western slope of the Olenek Uplift,  
1031 Siberian Platform. *Precambrian Research* 270, 226-245.
- 1032 Nagy, R.M., Porter, S.M., Dehler, C.M., Shen, Y., 2009. Biotic turnover driven by  
1033 eutrophication before the Sturtian low-latitude glaciation. *Nature Geosci* 2, 415-418.
- 1034 Pang, K., Tang, Q., Schiffbauer, J.D., Yao, J., Yuan, X., Wan, B., Chen, L., Ou, Z.,  
1035 Xiao, S., 2013. The nature and origin of nucleus-like intracellular inclusions in  
1036 Paleoproterozoic eukaryote microfossils. *Geobiology* 11, 499-510.

- 1037 Pang, K., Tang, Q., Yuan, X.-L., Wan, B., Xiao, S., 2015. A biomechanical analysis of  
1038 the early eukaryotic fossil *Valeria* and new occurrence of organic-walled microfossils  
1039 from the Paleo-Mesoproterozoic Ruyang Group. *Palaeoworld* 24, 251-262.
- 1040 Peat, C.J., Muir, M.D., Plumb, K.A., McKirdy, D.M., Norvick, M.S., 1978. Proterozoic  
1041 microfossils from the Roper Group, Northern Territory, Australia. *BMR Journal of*  
1042 *Australian Geology & Geophysics* 3, 1-17.
- 1043 Porter, S.M., Knoll, A.H., 2000. Testate amoebae in the Neoproterozoic Era:  
1044 evidence from vase-shaped microfossils in the Chuar Group, Grand Canyon.  
1045 *Paleobiology* 26, 360-385.
- 1046 Porter, S.M., Riedman, L.A., 2016. Systematics of organic-walled microfossils from  
1047 the ca. 780–740 Ma Chuar Group, Grand Canyon, Arizona. *Journal of Paleontology*  
1048 90, 815-853.
- 1049 Prasad, B., Asher, R., 2001. Acritarch Biostratigraphy and Lithostratigraphic  
1050 Classification of Proterozoic and Lower Paleozoic Sediments (Pre-Unconformity  
1051 Sequence) of Ganga Basin, In. *Paleontographica Indica* 5, 1-151.
- 1052 Riedman, L.A., Porter, S., 2016. Organic-walled microfossils of the mid-  
1053 Neoproterozoic Alinya Formation, Officer Basin, Australia. *Journal of Paleontology*  
1054 90, 854-887.
- 1055 Rooney, A.D., Selby, D., Houzay, J.-P., Renne, P.R., 2010. Re–Os geochronology of  
1056 a Mesoproterozoic sedimentary succession, Taoudeni basin, Mauritania: Implications  
1057 for basin-wide correlations and Re–Os organic-rich sediments systematics. *Earth and*  
1058 *Planetary Science Letters* 289, 486-496.



- 1059 Samuelsson, J., 1997. Biostratigraphy and palaeobiology of Early Neoproterozoic  
1060 strata of the Kola Peninsula, Northwest Russia. *Norsk Geologisk Tidsskrift* 77, 165-  
1061 192.
- 1062 Samuelsson, J., 1998. Carbon and oxygen isotope geochemistry of Early  
1063 Neoproterozoic successions on the Kola Peninsula, northwest Russia. *Norsk*  
1064 *Geologisk Tidsskrift* 78, 291-303.
- 1065 Samuelsson, J., Butterfield, N.J., 2001. Neoproterozoic fossils from the Franklin  
1066 Mountains, northwestern Canada: stratigraphic and palaeobiological implications.  
1067 *Precambrian Research* 107, 235-251.
- 1068 Samuelsson, J., Dawes, P.R., Vidal, G., 1999. Organic-walled microfossils from the  
1069 Proterozoic Thule Supergroup, Northwest Greenland. *Precambrian Research* 96, 1-  
1070 23.
- 1071 Schopf, J.W., Klein, C., 1992. *The Proterozoic Biosphere. A Multidisciplinary Study.*  
1072 Cambridge University Press, Cambridge.
- 1073 Semikhatov, M.A., Kuznetsov, A.B., Chumakov, N.M., 2015. Isotope age of  
1074 boundaries between the general stratigraphic subdivisions of the Upper Proterozoic  
1075 (Riphean and Vendian) in Russia: The evolution of opinions and the current estimate.  
1076 *Stratigraphy and Geological Correlation* 23, 568-579.
- 1077 Semikhatov, M.A., Ovchinnikova, G.V., Gorokhov, I.M., Kuznetsov, A.B., Vasil'eva,  
1078 I.M., Gorokhovskii, B.M., Podkovyrov, V.N., 2000. Isotopic Age of the Middle-Upper  
1079 Riphean Boundary: Pb-Pb Geochronology of the Lakhanda Group Carbonates,  
1080 Eastern Siberia. *Dokl. Earth Sc.* 372, 625-629.

- 1081 Sergeev, V.N., 2001. Paleobiology of the Neoproterozoic (Upper Riphean) Shorikha  
1082 and Burovaya silicified microbiotas, Turukhansk Uplift, Siberia. *Journal of*  
1083 *Paleontology* 75, 427-448.
- 1084 Sergeev, V.N., 2009. The distribution of microfossil assemblages in Proterozoic  
1085 rocks. *Precambrian Research* 173, 212-222.
- 1086 Sergeev, V.N., Knoll, A.H., Vorob'eva, N.G., Sergeeva, N.D., 2016. Microfossils from  
1087 the lower Mesoproterozoic Kaltasy Formation, East European Platform. *Precambrian*  
1088 *Research* 278, 87-107.
- 1089 Sergeev, V.N., Schopf, J.W., 2010. Taxonomy, Paleoecology and Biostratigraphy of  
1090 the Late Neoproterozoic Chichkan Microbiota of South Kazakhstan: The Marine  
1091 Biosphere on the Eve of Metazoan Radiation. *Journal of Paleontology* 84, 363-401.
- 1092 Shields, G.A., Deynoux, M., Strauss, H., Paquet, H., Nahon, D., 2007. Barite-bearing  
1093 cap dolostones of the Taoudéni Basin, northwest Africa: Sedimentary and isotopic  
1094 evidence for methane seepage after a Neoproterozoic glaciation. *Precambrian*  
1095 *Research* 153, 209-235.
- 1096 Stanevich, A.M., Kozlov, V.I., Puchkov, V.N., Kornilova, T.A., Sergeeva, N.D., 2012.  
1097 Paleobiocoenoses in the middle-upper riphean stratotype of the Southern Urals.  
1098 *Dokl. Earth Sc.* 446, 1059-1063.
- 1099 Tang, Q., Pang, K., Xiao, S., Yuan, X., Ou, Z., Wan, B., 2013. Organic-walled  
1100 microfossils from the early Neoproterozoic Liulaobei Formation in the Huainan region  
1101 of North China and their biostratigraphic significance. *Precambrian Research* 236,  
1102 157-181.

- 1103 Tang, Q., Pang, K., Yuan, X., Wan, B., Xiao, S., 2015. Organic-walled microfossils  
1104 from the Tonian Gouhou Formation, Huaibei region, North China Craton, and their  
1105 biostratigraphic implications. *Precambrian Research* 266, 296-318.
- 1106 Teal, D.A., Kah, 2005. Using C-isotopes to constrain intrabasinal stratigraphic  
1107 correlations: Mesoproterozoic Atar Group, Mauritania. *Geological Society of America,*  
1108 *Abstracts with Programs* p. 45.
- 1109 Thomson, D., Rainbird, R.H., Dix, G., 2014. Architecture of a Neoproterozoic  
1110 intracratonic carbonate ramp succession: Wynniatt Formation, Amundsen Basin,  
1111 Arctic Canada. *Sedimentary Geology* 299, 119-138.
- 1112 Timofeev, B.V., Hermann, T.N., Mikhailova, N.S., 1976. Mikrofitofossilii Dokembriya,  
1113 Kembriya i Ordovika [Microphytofossils of the Precambrian, Cambrian and  
1114 Ordovician]. Academy of Sciences, U.S.S.R., Institute Geology and Geochronology  
1115 of the Precambrian, Nauka.
- 1116 Trompette, R., 1973. Le Précambrien supérieur et le Paléozoïque inférieur de l'Adrar  
1117 de Mauritanie (bordure occidentale du bassin de Taoudeni, Afrique de l'Ouest). Un  
1118 exemple de sédimentation de craton. Étude stratigraphique et sédimentologique.  
1119 *Travaux des Laboratoires des Sciences de la Terre St-Jérôme, Marseille.* B-7, 702.
- 1120 Trompette, R., Carozzi, A.V., 1994. *Geology of Western Gondwana (2000-500 Ma).*  
1121 Balkema, A. A., Rotterdam.
- 1122 Turner, E.C., Kamber, B.S., 2012. Arctic Bay Formation, Borden Basin, Nunavut  
1123 (Canada): Basin evolution, black shale, and dissolved metal systematics in the  
1124 Mesoproterozoic ocean. *Precambrian Research* 208–211, 1-18.

- 1125 Veis, A.F., Petrov, P.Y., Vorob'eva, N.G., 1998. The Late Riphean Miroedikha  
1126 Microbiota from Siberia. Part 1: Composition and Facial-Ecological Distribution of  
1127 Organic-Walled Microfossils. *Stratigraphy and Geological Correlation* 6, 440-461.
- 1128 Vidal, G., 1976. Late Precambrian microfossils from the Visingsö beds, South  
1129 Sweden. *Fossils Strata* 9, 1-57.
- 1130 Vidal, G., 1981. Micropalaeontology and biostratigraphy of the Upper Proterozoic and  
1131 Lower Cambrian sequence in East Finnmark, northern Norway. *Norges geologiske*  
1132 *undersøkelse*.
- 1133 Vidal, G., Ford, T.D., 1985. Microbiotas from the late proterozoic chuar group  
1134 (northern Arizona) and uinta mountain group (Utah) and their chronostratigraphic  
1135 implications. *Precambrian Research* 28, 349-389.
- 1136 Vidal, G., Siedlecka, A., 1983. Planktonic, acid-resistant microfossils from the Upper  
1137 Proterozoic strata of the Barents Sea Region of Varanger Peninsula, East Finnmark,  
1138 Northern Norway. *Norges geologiske undersøkelse* 382, 45-79.
- 1139 Vorob'eva, N.G., Sergeev, V.N., Petrov, P.Y., 2015. Kotuikan Formation assemblage:  
1140 A diverse organic-walled microbiota in the Mesoproterozoic Anabar succession,  
1141 northern Siberia. *Precambrian Research* 256, 201 - 222.
- 1142 Waterbury, J.B., Stanier, R.Y., 1978. Patterns of Growth and Development in  
1143 Pleurocapsalean Cyanobacteria. *Microbiological Reviews* 42, 2-44.
- 1144 Xiao, S., Knoll, A.H., Kaufman, A.J., Yin, L., Zhang, Y., 1997. Neoproterozoic fossils  
1145 in Mesoproterozoic rocks? Chemostratigraphic resolution of a biostratigraphic  
1146 conundrum from the North China Platform. *Precambrian Research* 84, 197-220.

- 1147 Xiao, S., Shen, B., Tang, Q., Kaufman, A.J., Yuan, X., Li, J., Qian, M., 2014.  
1148 Biostratigraphic and chemostratigraphic constraints on the age of early  
1149 Neoproterozoic carbonate successions in North China. *Precambrian Research* 246,  
1150 208-225.
- 1151 Yin, L., 1997. Acanthomorphic acritarchs from Meso-Neoproterozoic shales of the  
1152 Ruyang Group, Shanxi, China. *Review of Palaeobotany and Palynology* 98, 15-25.
- 1153 Yin, L., Guan, B., 1999. Organic-walled microfossils of Neoproterozoic Dongjia  
1154 Formation, Lushan County, Henan Province, North China. *Precambrian Research* 94,  
1155 121 - 137.
- 1156 Yin, L., Yuan, X., Meng, F., Hu, J., 2005. Protists of the Upper Mesoproterozoic  
1157 Ruyang Group in Shanxi Province, China. *Precambrian Research* 141, 49-66.
- 1158 Zang, W.-l., 1995. Early Neoproterozoic sequence stratigraphy and acritarch  
1159 biostratigraphy, eastern Officer Basin, South Australia. *Precambrian Research* 74,  
1160 119-175.
- 1161 Zhang, Z., 1986. Clastic facies microfossils from the Chuanlinggou Formation (1800  
1162 Ma) near Jixian, North China. *Journal of Micropalaeontology* 5, 9-16.

1163

1164 **Figure legends**

1165 Figure 1 (2 column fitting image). Simplified geology of the Taoudeni Basin. Modified  
1166 from BEICIP (1981). Data from TOTAL (pers. comm., 2005). Locator map indicates  
1167 Mauritania (in grey) in Africa and the studied area (rectangle) described on the main  
1168 map.

1169 Figure 2 (1.5 column fitting image). Stratigraphy of Supergroups 1 (Hodh) and 2  
 1170 (Adrar) of the Taoudeni Basin. Modified after Rooney et al. (2010). Rb-Sr  
 1171 geochronology data from Clauer (1976, 1981; (Geboy, 2006)Clauer et al. (1982);  
 1172 Clauer and Deynoux (1987)). Re-Os geochronology datings from Rooney et al.  
 1173 (2010). Stratigraphic nomenclature after Trompette (1973) and Lahondère et al.  
 1174 (2003). Sinusoidal dashed lines represent unconformities noted D1, D2, D3, and D4  
 1175 (Lahondère et al., 2003). Linear dashed lines represent lateral changes.

1176 Figure 3 (1.5 column fitting image). Generalized lithostratigraphic column of the S2  
 1177 core - El Mreïti Group (Supergroup 1 - Hodh), Taoudeni Basin, Mauritania.

## 1178 **Plates**

1179 Plate 1. Each picture is described as following: species name\_slide number (ULg  
 1180 collection)\_and England Finder graticule coordinates (core, depth in m, formation,  
 1181 lithology). (a) *Arctacellularia tetragonala*\_63959\_R-26 (S2, 212.66-77m, Khatt  
 1182 Formation, green shale), (b) *Arctacellularia tetragonala*\_71631\_B-16-1 (S4, 132.29m,  
 1183 Unit I-4, dark-grey shale), (c) *Arctacellularia tetragonala*\_63959\_X-32-2 (S2, 212.66-  
 1184 77m, Khatt Formation, green shale), arrow (c) showing internal spheroidal inclusion,  
 1185 (d) *Arctacellularia tetragonala*\_63955\_J-45-2 (S2, 211.24-31m, Khatt Formation,  
 1186 green shale), (e) *Chlorogloeopsis contexta*\_72090\_N-20 (S4, Unit I-3, 161.91m,  
 1187 dark-grey shale), (f) *Chlorogloeopsis kanshiensis*\_63960\_O-37-4 (S2, 212.66-77m,  
 1188 Khatt Formation, green shale), (g) *Chlorogloeopsis zairensis*\_63512\_G-59-2 (S2,  
 1189 190.28-37, En Nesoar Formation, grey shale), (h) *Chuarina circularis*\_71571\_K-36-3  
 1190 (S3, 61.27m, Aguel el Mabha Formation, grey shale), (i) *Comasphaeridium*  
 1191 *tonium*\_63959\_J-35-1 (S2, 212.66-77m, Khatt Formation, green shale), (j-k)  
 1192 *Comasphaeridium tonium*\_63959\_R-31-1 (S2, 212.66-77m, Khatt Formation, green

1193 shale), (k) showing details of solid hair-like processes of specimen (j), (l) cf.  
 1194 *Coneosphaera* sp.\_63534\_K-36-1 (S2, 213.34-38m, Khatt Formation, green shale),  
 1195 (m) *Eomicrocystis irregularis*\_63766\_X-27-2 (S2, 78.71-76m, Aguel el Mabha  
 1196 Formation, green shale), (n) *Eomicrocystis malgica*\_63906\_M-45-4 (S2, 157.67-77m,  
 1197 Tourist Formation, green shale), (o) *Gemmulooides doncookii*\_63959\_P-46 (S2,  
 1198 212.66-77m, Khatt Formation, green shale), (p) *Jacutianema solubila* (morphotype-  
 1199 1)\_63959\_J-39-3 (S2, 212.66-77m, Khatt Formation, green shale), (q) *Jacutianema*  
 1200 *solubila* (morphotype-1)\_63959\_M-52-3 (S2, 212.66-77m, Khatt Formation, green  
 1201 shale), (r) *Jacutianema solubila* (morphotype-2)\_72035\_R-18-4 (S4, 128.06m, Unit I-  
 1202 4, dark-grey shale), arrow in (r) showing constriction, (s) *Jacutianema solubila*  
 1203 (morphotype-3)\_72035\_M-29 (S4, 128.06m, Unit I-4, dark-grey shale), (t)  
 1204 *Jacutianema solubila* (morphotype-4)\_63959\_V-56 (S2, 212.66-77m, Khatt  
 1205 Formation, green shale), (u) *Jacutianema solubila* (morphotype-5)\_63959\_P-41-1  
 1206 (S2, 212.66-77m, Khatt Formation, green shale).

1207 Plate 2. Each picture is described as following: species name\_slide number (ULg  
 1208 collection)\_and England Finder graticule coordinates (core, depth in m, formation,  
 1209 lithology). (a-b) *Leiosphaeridia atava*\_63493\_S-53-2 (S2, 104.89-93m, Aguel el  
 1210 Mabha Formation, green shale), (b) showing details of finely granulate texture of  
 1211 specimen (a) , (c) *Leiosphaeridia crassa*\_63885\_V-46-4 (S2, 194.18-25m, En Nesoar  
 1212 Formation, dark-grey shale), (d) Excystment structure *Leiosphaeridia*  
 1213 *crassa*\_63534\_D-26-2 (S2, 213.34-38m, Khatt Formation, green shale), (e)  
 1214 *Leiosphaeridia jacutica*\_63512\_V-38-4 (S2, 190.28-37, En Nesoar Formation, grey  
 1215 shale), (f) *Leiosphaeridia kulgunica*\_71575-K-44 (S3, 123.37m, Aguel el Mabha  
 1216 Formation, grey shale), white arrow in (f) showing circular opening edge, (g)  
 1217 *Leiosphaeridia minutissima*\_63885\_T-48-4 (S2, 194.18-25m, En Nesoar Formation,



1218 dark-grey shale), (h) Excystment structure *Leiosphaeridia minutissima*\_63881\_R-58-  
 1219 3 (S2, 191.30-39m, En Nesoar Formation, grey shale), (i) *Leiosphaeridia*  
 1220 *obsuleta*\_63493\_Y-42-2 (S2, 104.89-93m, Aguel el Mabha Formation, green shale),  
 1221 (j) *Leiosphaeridia tenuissima*\_63879\_K-42-3 (S2, 189.46-54m, En Nesoar Formation,  
 1222 grey-green shale), (k) *Leiosphaeridia ternata*\_63879\_M-25 (S2, 189.46-54m, En  
 1223 Nesoar Formation, grey-green shale), (l) *Leiosphaeridia* sp. surrounded by an outer  
 1224 membrane\_63959\_O-40-1 (S2, 212.66-77m, Khatt Formation, green shale), arrow in  
 1225 (i) showing the outer membrane, (m) *Navifusa actinomorpha*\_63885\_S-36-4 (S2,  
 1226 194.18-25m, En Nesoar Formation, dark-grey shale), (n) *Navifusa*  
 1227 *majensis*\_63959\_S-20 (S2, 212.66-77m, Khatt Formation, green shale), (o-p)  
 1228 Microbial mats with pyritized filaments\_63932\_H-36 (S2, 198.43-50m, En Nesoar  
 1229 Formation, green and black shale), (p) showing details of microbial mats in (o), (q)  
 1230 *Obruchevella* sp.\_63514\_W-44-1 (S2, 193.25-28m, En Nesoar Formation, grey and  
 1231 black shale), (r) *Obruchevella* sp.\_63534\_J-32-4 (S2, 213.34-38m, Khatt Formation,  
 1232 green shale), (s) *Ostiana microcystis*\_63959\_X-49 (S2, 212.66-77m, Khatt  
 1233 Formation, green shale), (t) *Pellicularia tenera*\_63959\_G-44 (S2, 212.66-77m, Khatt  
 1234 Formation, green shale), (u) *Polysphaeroides* sp.\_71601\_W-25-1 (S4, 79.43m, Unit I-  
 1235 5, dark-grey shale).

1236 Plate 3. Each picture is described as following: species name\_slide number (ULg  
 1237 collection)\_and England Finder graticule coordinates (core, depth in m, formation,  
 1238 lithology). (a) *Polytrichoides lineatus*\_63536\_V-19-1 S2, 216.29-34m, Khatt  
 1239 Formation, dark-grey shale), (b) *Pterospermopsimorpha insolita*\_63695\_D-39 (S2,  
 1240 75.53-59m, Aguel el Mabha Formation, green and red shale), (c)  
 1241 *Pterospermopsimorpha insolita*\_63638\_D-28 (S2, 72.10-16m, Aguel el Mabha  
 1242 Formation, green shale), (d) *Pterospermopsimorpha pileiformis*\_71625\_O-33 (S4,

1243 91.16m, Unit I-5, dark-grey shale), (e) *Simia annulare*\_63526\_R-44 (S2, 199.76-84m,  
 1244 En Nesoar Formation, green shale), (f) *Siphonophycus gigas*\_72033\_E-34 (S4,  
 1245 122.78m, Unit I-4, dark-grey shale), (g) *Siphonophycus kestron*\_71625\_O-33-2 (S4,  
 1246 91.16m, Unit I-5, dark-grey shale), (h) *Siphonophycus punctatum*\_72033\_K-29 (S4,  
 1247 122.78m, Unit I-4, dark-grey shale), (i) *Siphonophycus robustum*\_63959\_G-34-4 (S2,  
 1248 212.66-77m, Khatt Formation, green shale), (j) *Siphonophycus septatum*\_71920\_C-  
 1249 17 (S2, 138.9m, Tourist Formation, green shale), (k) *Siphonophycus*  
 1250 *solidum*\_71920\_R-22 (S2, 138.9m, Tourist Formation, green shale), (l)  
 1251 *Siphonophycus thulenema*\_71920\_C-18-1 (S2, 138.9m, Tourist Formation, green  
 1252 shale), (m) *Siphonophycus thulenema*\_63955\_U-32-1 (S2, 211.24-31m, Khatt  
 1253 Formation, green shale), (n) *Siphonophycus typicum*\_63959\_N-52-1 (S2, 212.66-  
 1254 77m, Khatt Formation, green shale), (o) *Spiromorpha segmentata*\_63534\_J-39 (S2,  
 1255 213.34-38m, Khatt Formation, green shale), (p) *Spiromorpha segmentata*\_63534\_G-  
 1256 50 (S2, 213.34-38m, Khatt Formation, green shale), (q) *Spumosina*  
 1257 *rubiginosa*\_63532\_F-35-1 (S2, 211.59-6m, Khatt Formation, green shale), (r)  
 1258 *Synsphaeridium* sp.\_63879\_Q-23-3 (S2, 189.46-54m, En Nesoar Formation, grey-  
 1259 green shale), (s) *Synsphaeridium* sp.\_63858\_M-28 (S2, 146.74-80m, Tourist  
 1260 Formation, green and brown shale), (t) *Tortunema patomica*\_71604\_K-33-3 (S4,  
 1261 81.42m, Unit I-5, dark-grey shale), (u) *Tortunema wernadskii*\_63532\_E-34-4 (S2,  
 1262 211.59-6m, Khatt Formation, green shale), (v) *Trachyhystrichosphaera*  
 1263 *aimika*\_71979\_W-23 (S2, 188.6m, En Nesoar Formation, green shale), arrow in (v)  
 1264 showing tubular hollow process.

1265 Plate 4. Each picture is described as following: species name\_slide number (ULg  
 1266 collection)\_and England Finder graticule coordinates (core, depth in m, formation,  
 1267 lithology). (a-c) *Trachyhystrichosphaera aimika*\_63526\_R-51-3 (S2, 199.76-84m, En

1268 Nesoar Formation, green shale), arrows in (b-c) showing details of hollow processes  
1269 in (a), (d-e) *Trachyhystrichosphaera aimika\_63936\_V-31* (S2, 199.67-70m, En  
1270 Nesoar Formation, grey shale), (e) showing details of the specimen in (d), arrows in  
1271 (d-e) showing details of hollow processes, (f-i) *Trachyhystrichosphaera*  
1272 *botula\_71979\_N-36* (S2, 188.6m, En Nesoar Formation, green shale), arrows in (g-i)  
1273 showing details of processes in (f), (j-k) *Valeria lophostriata\_63879\_U-39* (S2,  
1274 189.46-54m, En Nesoar Formation, grey-green shale), (k) showing details of thin  
1275 concentric striations in specimen 4j, (l) *Vidaloppala* sp. *\_63881\_R-58-4* (S2, 191.30-  
1276 39m, En Nesoar Formation, grey shale), (m-n) Unnamed form A *\_63959\_G-35-3* (S2,  
1277 212.66-77m, Khatt Formation, green shale), arrows in (n) showing details on spiny  
1278 ornamentation of the specimen in (m), (o-p) Unnamed form B *\_63959\_H-24* (S2,  
1279 212.66-77m, Khatt Formation, green shale), (p) showing details on verrucae of the  
1280 specimen in (o).

## 1281 **Tables**

1282 Table 1. Atar/EI Mreïti group organic-walled microfossils and inferred biological  
1283 affinities of each species: eukaryotes (E), incertae sedis (possible prokaryotes or  
1284 eukaryotes).

1285 Table 2. Occurrence of the Atar/EI Mreïti Group organic-walled microfossils in 24  
1286 geological localities between late Palaeoproterozoic to late Cryogenian at a  
1287 worldwide (global) scale. Only the 46 identified species are listed here. Bold localities  
1288 show high similarity with the Atar/EI Mreïti Group assemblage.

## 1289 **Supplementary Figure**

1290 Supplementary Figure 1A. Stratigraphic occurrence of the Atar/EIMreïti Group  
1291 species in S2 core.

1292 Supplementary Figure 1B Stratigraphic occurrence of the Atar/EIMreïti Group species  
1293 in S2 core.

1294 Supplementary Figure 2 Stratigraphic occurrence of the Atar/EIMreïti Group species  
1295 in S3 core.

1296 Supplementary Figure 3 Stratigraphic occurrence of the Atar/EIMreïti Group species  
1297 in S4 core.

### 1298 **Supplementary Table**

1299 Supplementary Table 1. Species reported in previous studies on the Taoudeni Basin.  
1300 In bold species reported in this study.

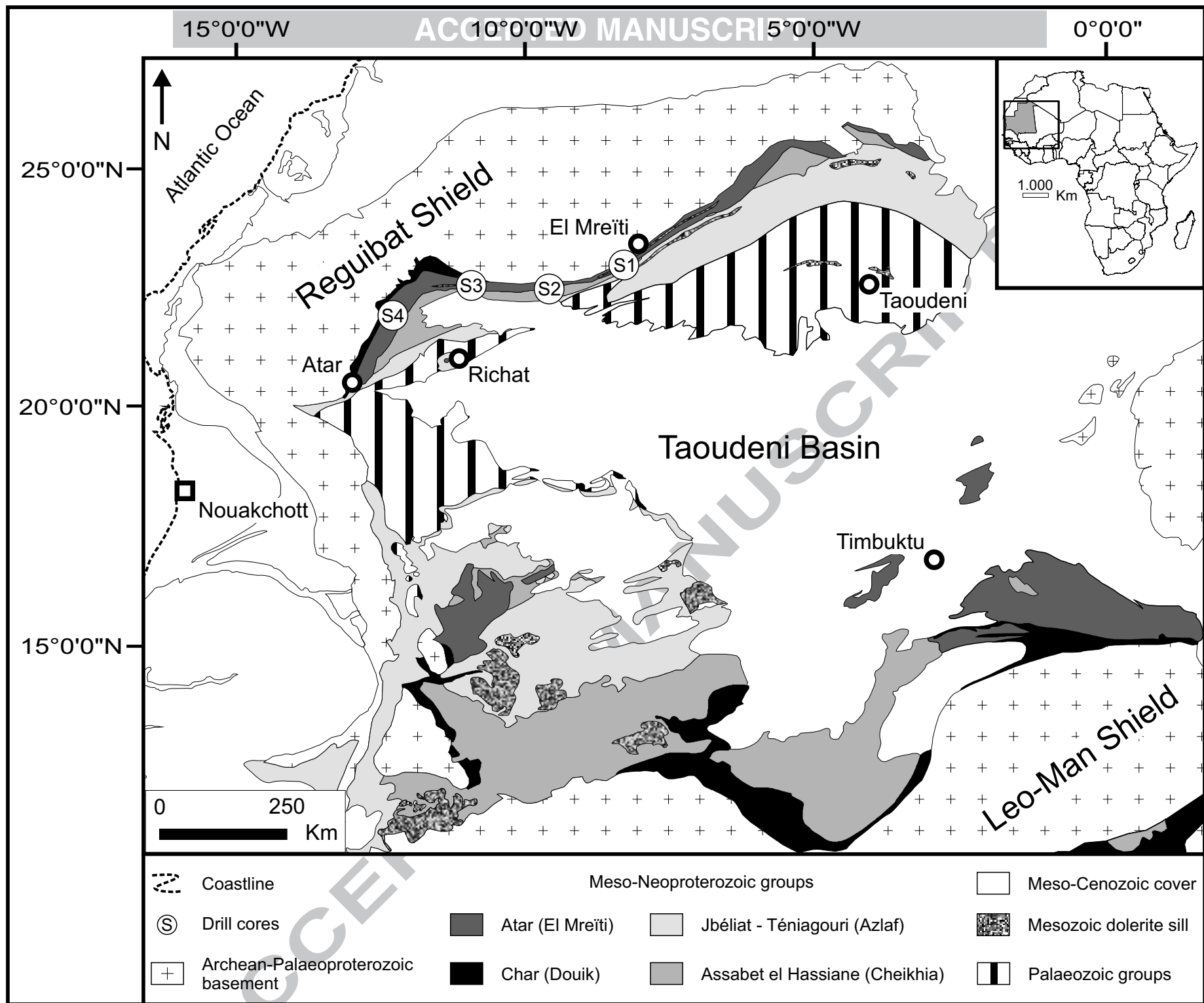
### 1301 **Supplementary data Caption Table 2**

1302 Occurrence (presence-absence) of the Atar/El Mreïti Group microfossils in 24  
1303 geological localities (groups, formations, units, sections and/or strata) between late  
1304 Palaeoproterozoic to late Cryogenian at a worldwide (global) scale. In the table, the  
1305 black dot (●) means: presence of the species. Geological localities: 1. 1750-1400 Ma  
1306 (U–Pb detrital zircons), Ruyang Group, China, (Xiao et al., 1997; Yin et al., 1997,  
1307 2005; Pang et al., 2015); 2. 1500-1450 Ma (Sm/Nd isotopic data on dyke and sills,  
1308 K/Ar and Rb/Sr on glauconite), Kotuikan, Formation, Billyakh Group, Russia  
1309 (Golovenok and Belova, 1984; Sergeev et al., 1995; Vorob'eva et al., 2015); 3. 1500-  
1310 1450 Ma (U–Pb zircons, Re-Os on shale and Rb-Sr on illite), Roper Group, Australia  
1311 (Javaux et al., 2001, 2003, 2004; Javaux and Knoll, in press); 4. 1499 ± 43 (Ar-Ar) to  
1312 1060 ± 20 (K-Ar) Ma, Yurubchen and 1526-1275 (Rb-Sr) Ma to 1265-1105 (K-Ar) Ma  
1313 Dzhelindukon formations, Kamo Group, Central Angara Basin, Siberian Craton,  
1314 Russia (Nagovitsin, 2009); 5. ~1350-1250 Ma, Sarda Formation, India (Prasad and

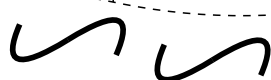
1315 Asher, 2001); 6. ~1300-1200 Ma, Thule Supergroup, Greenland (Samuelsson et al.,  
1316 1999). Note that Samuelsson et al. (1999) identified *Simia annulare* but to our view  
1317 the description refers to the genus *Pterospermopsimorpha*. They observed both  
1318 smooth and fine-granular outer vesicles. However, the available illustrations do not  
1319 allow to clearly identified the species and therefore occurrences are not reported  
1320 here; 7. 1092±59 Ma , Bylot Supergroup, Canada (Hofmann and Jackson, 1994;  
1321 Kah et al., 2001; Turner and Kamber, 2012); 8. ~1250-1150 Ma, Avadh Formation,  
1322 India (Prasad and Asher, 2001); 9. ~1100-850 Ma, Bushimay Supergroup,  
1323 Democratic Republic of the Congo (Zaire) (Baludikay et al., 2016; François et al.,  
1324 2015 for datings); 10. 1025 ± 40 Ma (Pb-Pb on limestone), Lakhanda Group, Russia  
1325 (Jankauskas et al., 1989; Hermann, 1990; Hermann and Podkovyrov, 2010;  
1326 Semikhatov et al., 2000, 2015); 11. ~1000-800 Ma, Mirojedikha Formation, Russia  
1327 (Jankauskas et al., 1989; Hermann, 1990); 12. ~1000-811 Ma or 840 ± 72 Ma (Rb-  
1328 Sr) but poorly constrained, Liulaobei Formation, China (Tang et al., 2013); 13. ~1000-  
1329 811 Ma or <1069 ± 27 Ma (detrital zircons), Gouhou Formation, China (Xiao et al.,  
1330 2014; Tang et al., 2015); 14. ~1000 Ma, Shorikha and Burovaya Formation, Russia  
1331 (Sergeev, 2001); 15. Neoproterozoic Lone Land Formation, Canada (Samuelsson  
1332 and Butterfield, 2001); 16. Neoproterozoic (<1.05 Ga, detrital zircon) G-52, Franklin  
1333 Mountains, northwestern Canada (Samuelsson and Butterfield, 2001); 17., ~ 850-800  
1334 Ma Browne, 926 ± 25-777 ± 7 Ma (U-Pb detrital zircon) Hussar and 777 ± 7 or 725 ±  
1335 11 (U-Pb detrital zircon) Kanpa formations, Supersequence 1, Australia (Cotter,  
1336 1999; Hill et al., 2000; Grey et al., 2005); 18. 850-750 Ma, Wynniatt Formation,  
1337 Canada (Butterfield and Rainbird, 1998; Samuelsson and Butterfield, 2001;  
1338 Butterfield, 2005); 19. ~820 Ma (<811.5-788 Ma,  $\delta^{13}\text{C}_{\text{carb}}$ ), Svanbergfjellet Formation,  
1339 Norway (Butterfield et al., 1994; Butterfield, 2004; 2015); 20. ~811-716.5 Ma, Alinya

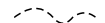
- 1340 Formation, Australia (Riedman and Porter, 2016); 21. ~800-750 Ma, Chichkan  
1341 Formation, Kazakhstan (Sergeev and Schopf, 2010); 22. 800-700 Ma, Draken  
1342 Conglomerate Formation, Norway (Knoll et al., 1991) 23. 780-740 Ma; 782 Ma (U-Pb  
1343 detrital zircon) and  $742 \pm 6$  Ma (U-Pb zircon), Chuar Group, USA (Porter and  
1344 Riedman, 2016); 24. >610 to >590 Ma, Scotia Group, Norway (Knoll, 1992).
- 1345

ACCEPTED MANUSCRIPT





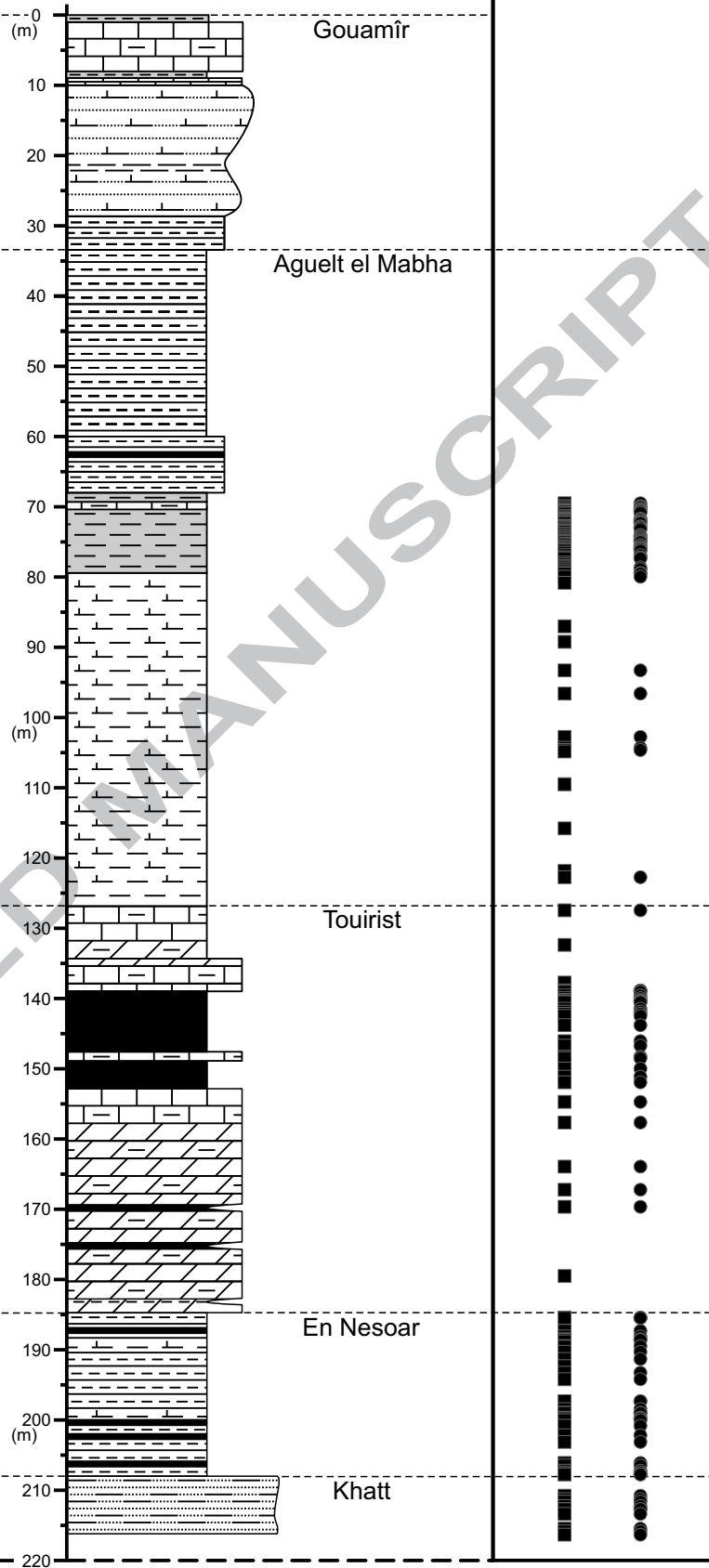
	Group	Unit / Formation		Rb-Sr date	Re-Os date	
		Trompette, 1973	Lahondère et al., 2003			
Supergroup 2 Adrar	Jbéliat		<i>Not subdivided</i>	630-595 Ma		
Supergroup 1 Hodh	Assabet el Hassiane / Cheikhia	I18				
		I17	Zreigât			
		I15-I16	Taguilalet	>694 Ma		
		I13-I14	Ti-n-Bessaïs			
	Atar / El Mreïti	I12				
		I11	Elb Nous			
		I10		775 ± 52 Ma		
		I9				
		I8	Ligdam		866 ± 67 Ma	
		I7	Tenoumer			
		I6	Gouamîr		874 ± 22 Ma	
			Aguelt el Mabha			
	I5	Tourist	890 ± 35 Ma	1105 ± 37 Ma 1107 ± 12 Ma 1109 ± 22 Ma		
	I4	En Nesoar				
I3	Khatt					
Char / Douik	I2	Chegga	998 ± 32 Ma			
	I1	Glebet el Atores				
	++					
	++		++			
	++		++			

+ + Archean-Palaeoproterozoic basement  
 Unconformities noted D1, D2, D3, and D4

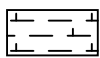
## Supergroup 1 - Hodh

## Group - El Mreïti

## Lithostratigraphy - Formation



Shale



Calcareous Shale



Rock samples



Black Shale



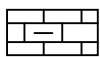
Calcareous Silt/Sandstone



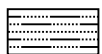
Fossiliferous samples



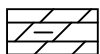
Shale/Siltstone



Shaley Limestone

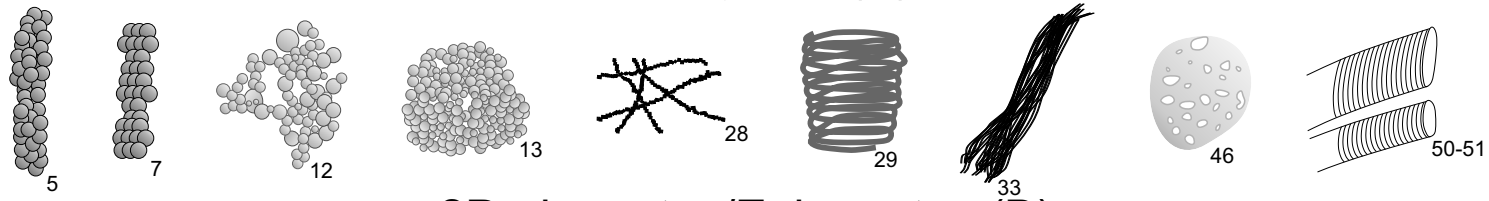


Silty/Sandy Shale

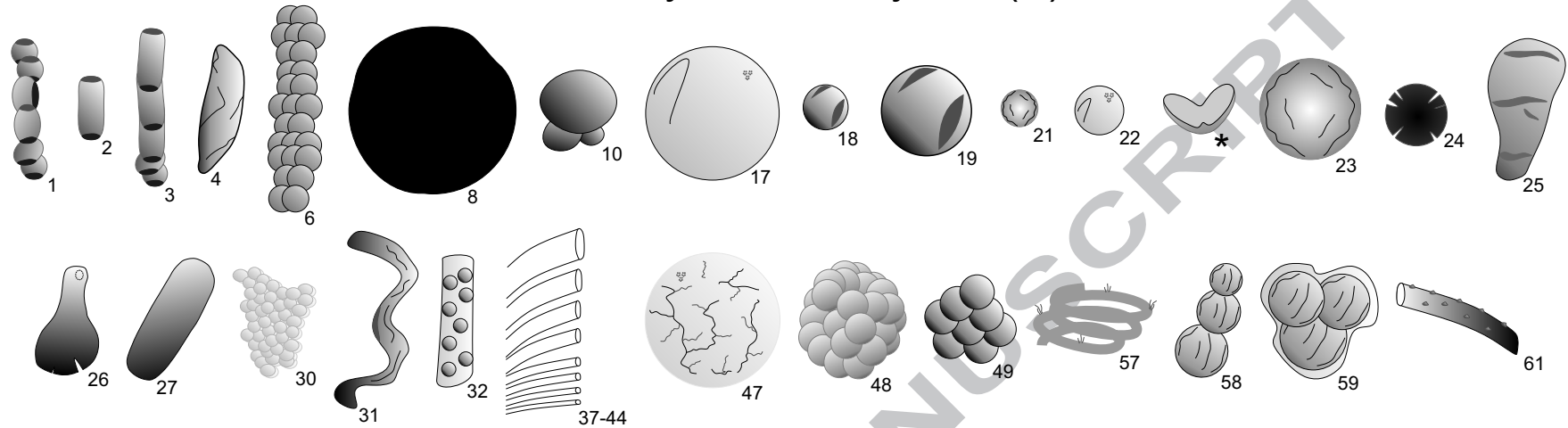


Shaley Dolomite

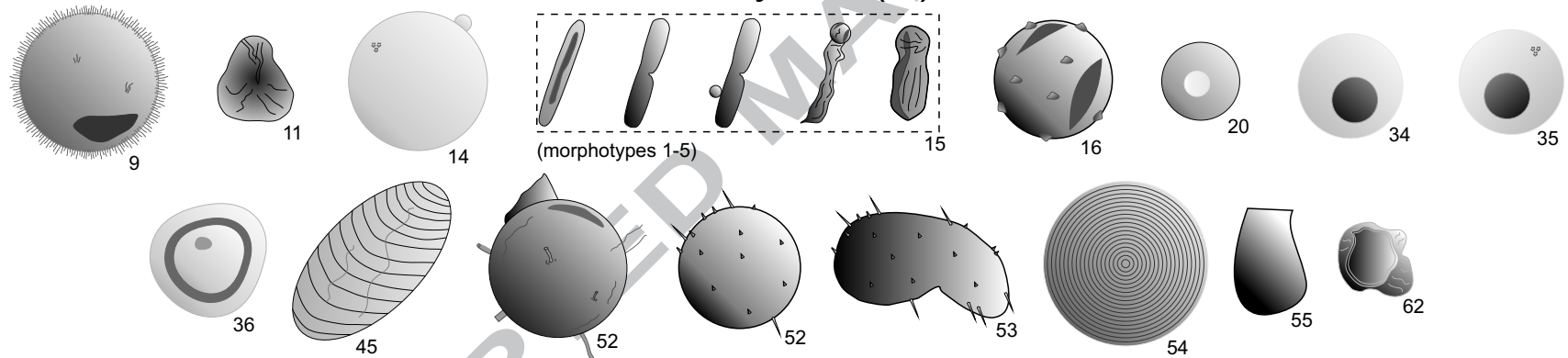
## Prokaryotes (A)



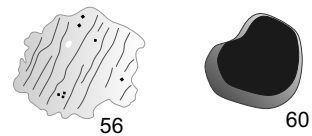
## ?Prokaryotes/Eukaryotes (B)



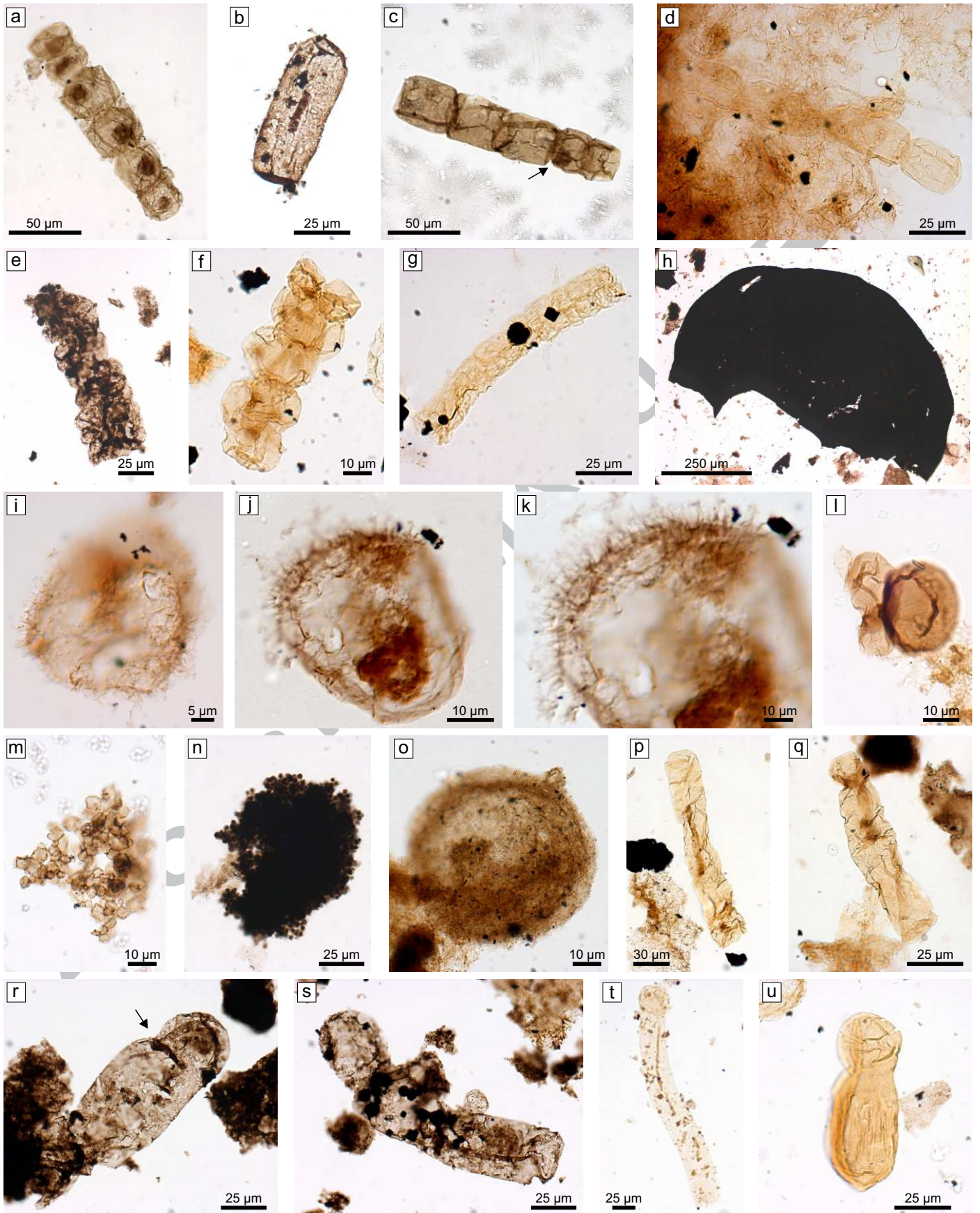
## Eukaryotes (C)



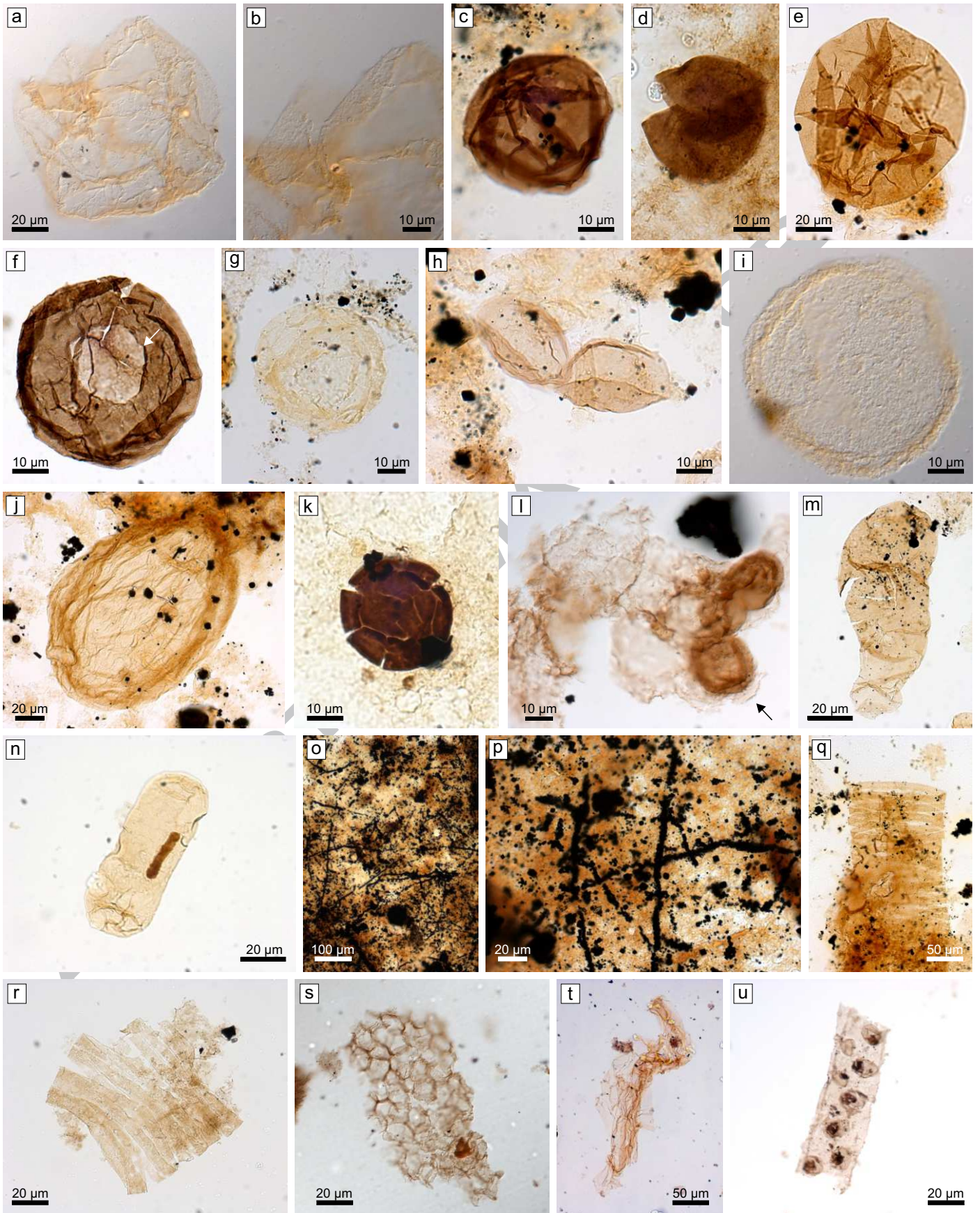
## Remains of structured kerogen (D)



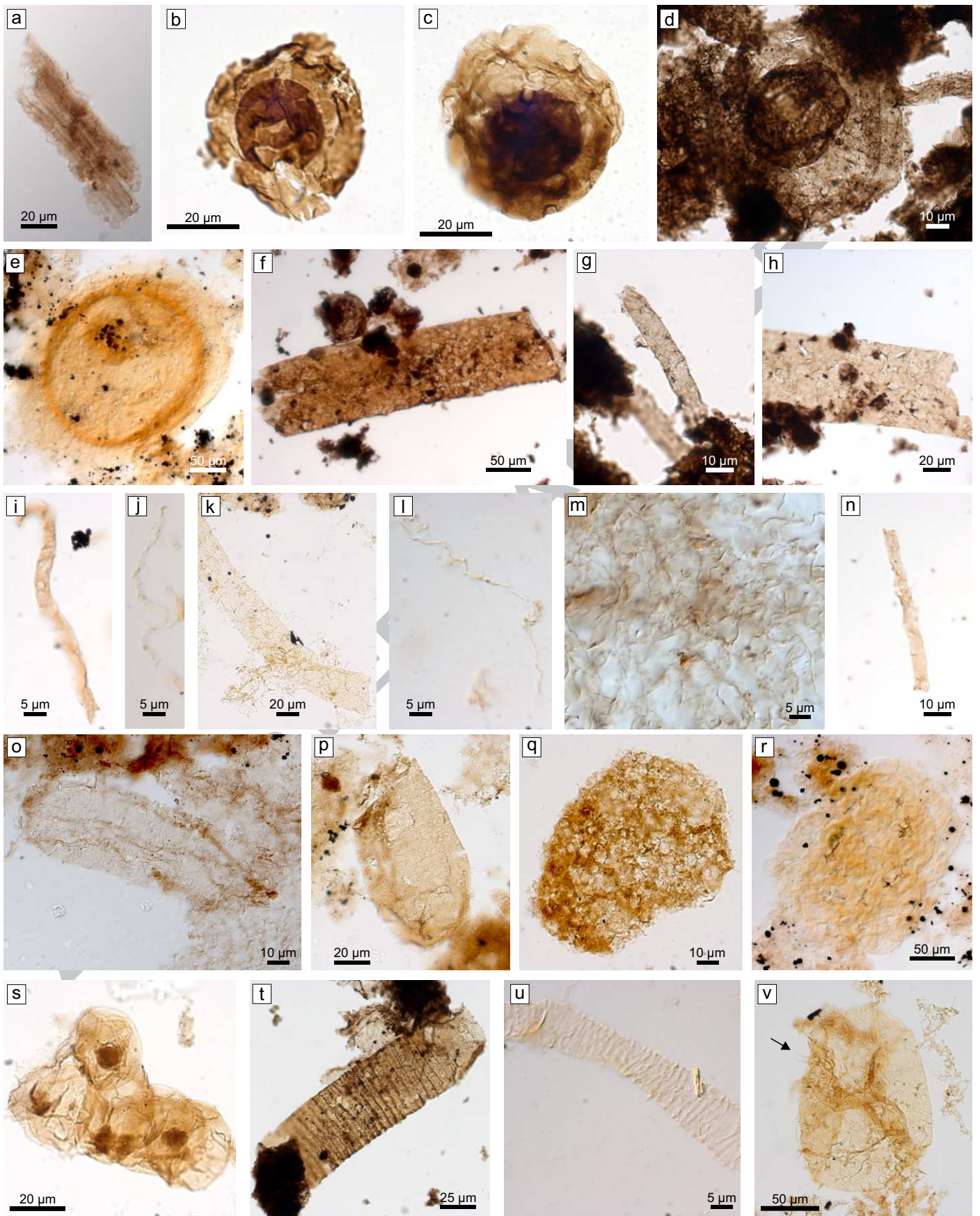
Not to scale.



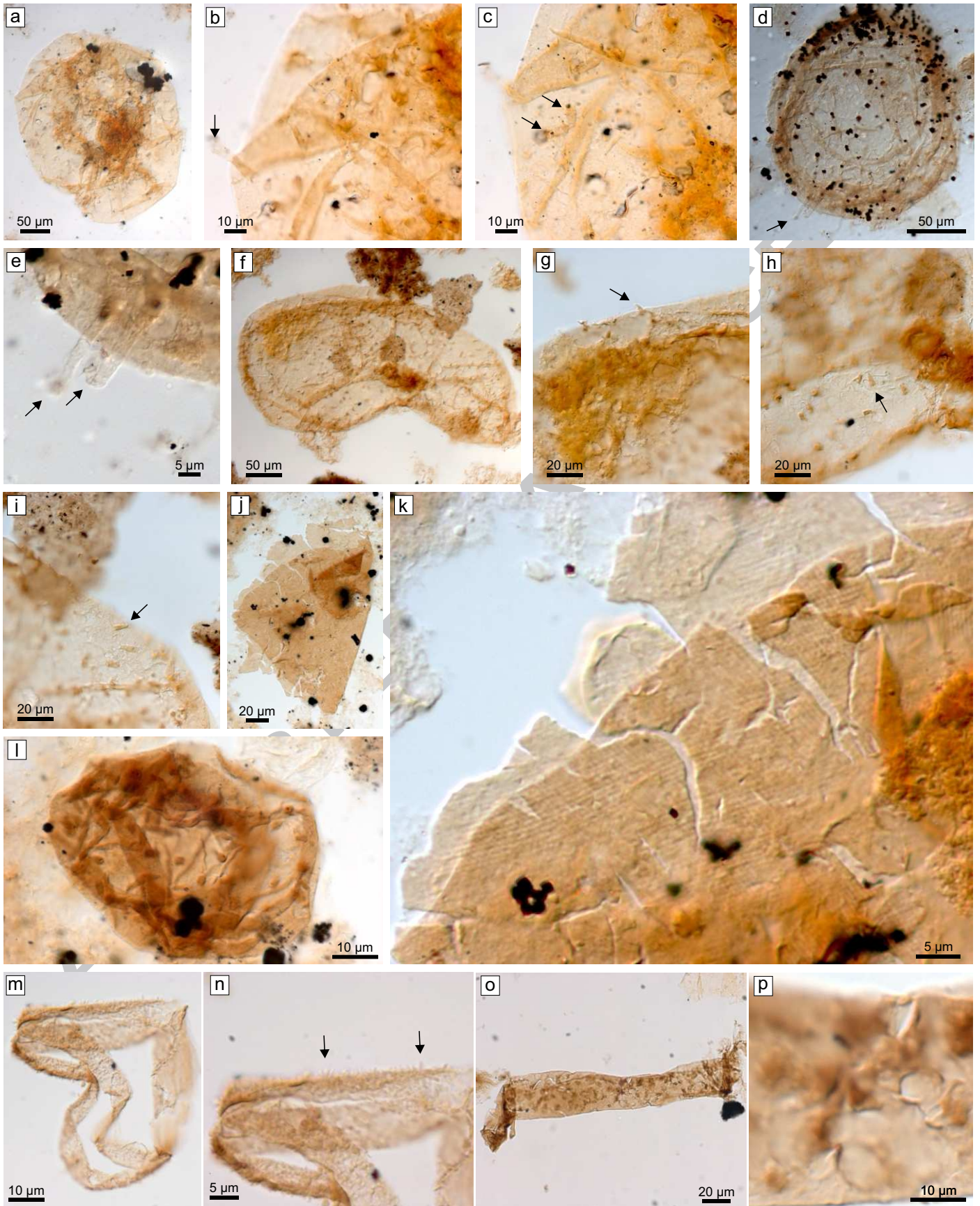




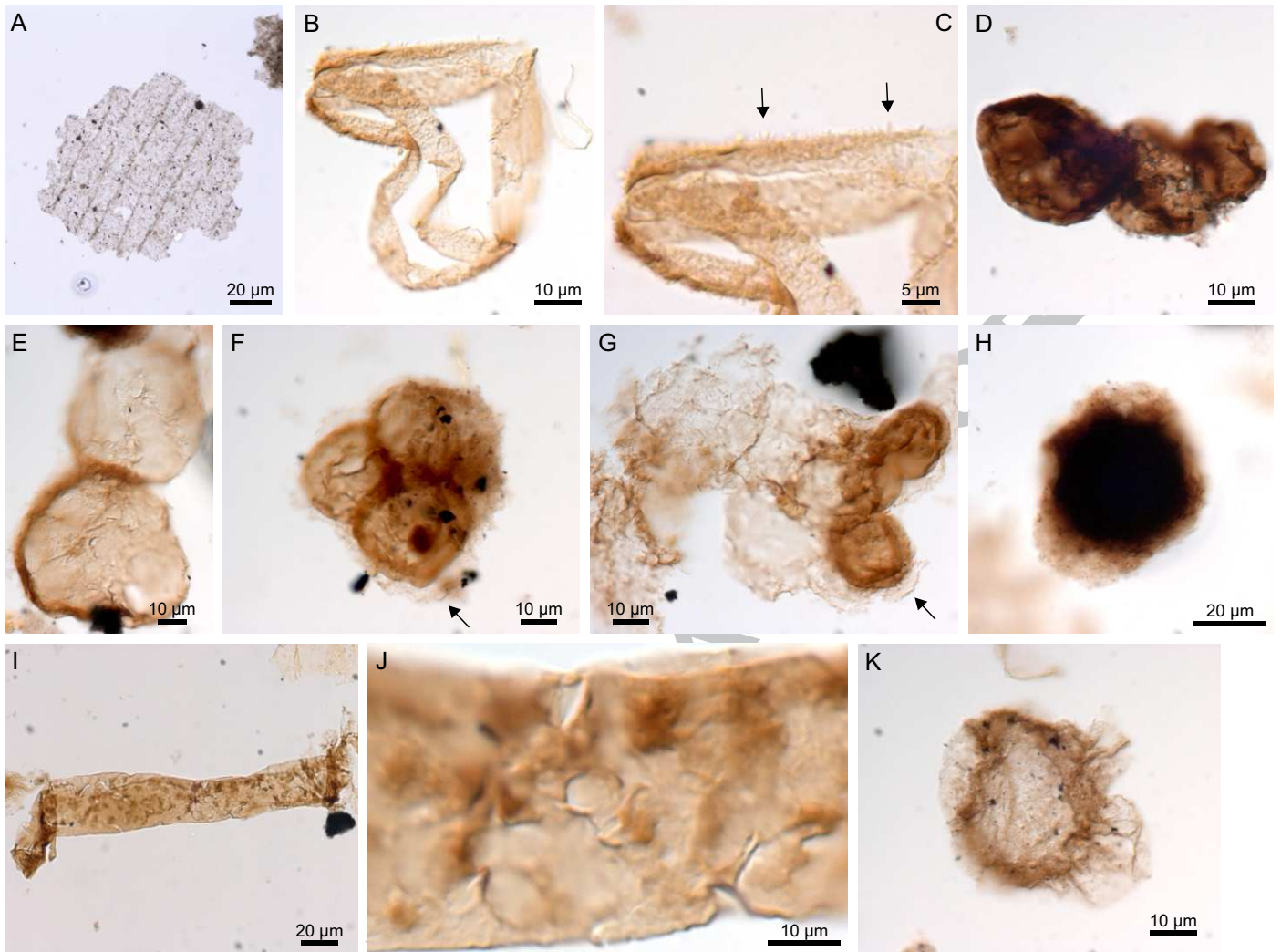












ACCEPTED



	Atar/EI Mreiti organic-walled microfossils	E	Incertae sedis	Plate
1	<i>Arctacellularia tetragonala</i>		•	1, a-d
2	<i>Chlorogloeopsis contexta</i>		•	1, e
3	<i>Chlorogloeopsis kanshiensis</i>		•	1, f
4	<i>Chlorogloeopsis zairensis</i>		•	1, g
5	<i>Chuarua circularis</i>		•	1, h
6	<i>Comasphaeridium tonium</i>	•		1, i-k
7	cf. <i>Coneosphaera</i> sp.		•	1, l
8	<i>Eomicrocystis irregularis</i>		•	1, m
9	<i>Eomicrocystis malgica</i>		•	1, n
10	<i>Gemmulooides doncookii</i>		•	1, o
11	<i>Jacutianema solubila</i> (morphotypes 1-5)	•		1, p-u
12	<i>Leiosphaeridia atava</i>		•	2, a and b
13	<i>Leiosphaeridia crassa</i>		•	2, c and d
14	<i>Leiosphaeridia jacutica</i>		•	2, e
15	<i>Leiosphaeridia kulgunica</i>	•		2, f
16	<i>Leiosphaeridia minutissima</i>		•	2, g and h
17	<i>Leiosphaeridia obsuleta</i>		•	2, i
18	<i>Leiosphaeridia tenuissima</i>		•	2, j
19	<i>Leiosphaeridia ternata</i>		•	2, k
20	<i>Navifusa actinomorpha</i>		•	2, m
21	<i>Navifusa majensis</i>		•	2, n
22	<i>Obruchevella</i> spp.		•	2, q and r
23	<i>Ostiana microcystis</i>		•	2, s
24	<i>Pellicularia tenera</i>		•	2, t
25	<i>Polysphaeroides</i> sp.		•	2, u
26	<i>Polytrichoides lineatus</i>		•	3, a
27	<i>Pterospermopsimorpha insolita</i>	•		3, b and c
28	<i>Pterospermopsimorpha pileiformis</i>	•		3, d
29	<i>Simia annulare</i>	•		3, e
30	<i>Siphonophycus gigas</i> (64-128 $\mu$ m)		•	3, f
31	<i>Siphonophycus kestron</i> (8-16 $\mu$ m)		•	3, g
32	<i>Siphonophycus punctatum</i> (32-64 $\mu$ m)		•	3, h
33	<i>Siphonophycus robustum</i> (2-4 $\mu$ m)		•	3, i
34	<i>Siphonophycus septatum</i> (1-2 $\mu$ m)		•	3, j
35	<i>Siphonophycus solidum</i> (16-32 $\mu$ m)		•	3, k
36	<i>Siphonophycus thulenema</i> (0.5 $\mu$ m)		•	3, l and m
37	<i>Siphonophycus typicum</i> (4-8 $\mu$ m)		•	3, n
38	<i>Spiromorpha segmentata</i>	•		3, o and p
39	<i>Spumosina rubiginosa</i>		•	3, q
40	<i>Synsphaeridium</i> spp.		•	3, r and s
41	<i>Tortunema patomica</i> (25-60 $\mu$ m)		•	3, t
42	<i>Tortunema wernadskii</i> (10-25 $\mu$ m)		•	3, u
43	<i>Trachyhystrichosphaera aimika</i>	•		3, v; 4 a-e
44	<i>Trachyhystrichosphaera botula</i>	•		4, f-i
45	<i>Valeria lophostriata</i>	•		4, j and k
46	<i>Vidaloppala</i> sp.	•		4, l
47	Unnamed form A (spiny filamentous sheath)		•	4, m and

48	Unnamed form B (verrucate filamentous sheath)	•	n 4, o and p
#	Microbial mats with pyritized filaments	•	2, o and p

ACCEPTED MANUSCRIPT

<i>Atar/Ei Mreiti</i> <i>organic-walled</i> <i>microfossils</i> <i>Arctacellularia</i> <i>tetragonala</i> <i>Chlorogloeaopsis</i> <i>contexa</i> <i>Chlorogloeaopsis</i> <i>kanshiensis</i> <i>Chlorogloeaopsis</i> <i>zatreensis</i> <i>Chuaria circularis</i> <i>Comasphaeridium</i> <i>m. tonium</i> <i>cf. Coneosphaera</i> <i>sp.</i> <i>Eomicrocystis</i> <i>irregularis</i> <i>Eomicrocystis</i> <i>malgica</i> <i>Gemmuloides</i> <i>doncockii</i> <i>Jacutianema</i> <i>sulbilla</i> <i>Leiosphaeridia</i> <i>atava</i>		Geological localities
		1750-1400 Ma, Ruyang Gr., China (Xiao et al., 1997; Yin et al., 1997, 2005; Pang et al., 2015) 1
		1500-1450 Ma, Kotuikan Fm., Russia (Sergeev et al., 1995; Vorob'eva et al., 2015) 2
		1500-1450 Ma, Roper Gr., Australia (Javaux et al., 2001, 2003, 2004; Javaux and Knoll, in press) 3
		~1500-1050 Ma, Kamo Gr., Russia (Nagovitsin, 2009) 4
		~1350-1250 Ma, Sarda Fm., India (Prasad and Asher, 2001) 5
		~1300-1200 Ma, Thule Supergr., Greenland (Samuelsson et al., 1999) 6
		~1250-1150 Ma, Avadh Fm., India (Prasad and Asher, 2001) 7
		<b>~1100-850 Ma, Mbuji-Mayi (Bushimay) Supergr., DRC (Baludikay et al., 2016) 8</b>
		<b>1092 ± 59 Ma, Bylot Supergr., Canada (Hofmann and Jackson, 1994) 9</b>
		1025 ± 40 Ma, Lakhanda Gr., Russia (Hermann, 1990) 10
		<b>~1000-811 Ma, Liulaobei Fm., China (Tang et al., 20013) 11</b>
		~1000-811 Ma, Gouhou Fm., China (Xiao et al., 2014; Tang et al., 2015) 12
		~1000 Ma, Shorikha and Burovaya Fm., Russia (Sergeev, 2001) 13
		<b>~1000-800 Ma, Mirojedikha Fm., Russia (Hermann, 1990) 14</b>
		Neoproterozoic, Lone Land Fm., Canada (Samuelsson and Butterfield, 2001) 15
		Neoproterozoic (<1.05 Ga) G-52, Canada (Samuelsson and Butterfield, 2001) 16
		~850-800 Ma, Browne, Supersequence 1, Australia (Cotter, 1999; Hill et al., 2000; Grey et al., 2005) 17
		~850-800 Ma, Hussar, Supersequence 1, Australia (Cotter, 1999; Hill et al., 2000; Grey et al., 2005) 18
		~800 Ma, Kanpa, Supersequence 1, Australia (Cotter, 1999; Hill et al., 2000; Grey et al., 2005) 19
		850-750 Ma, Wynniatt Fm., Canada (Samuelsson and Butterfield, 2001) 20
		<811.5-788 Ma, Svanbergfjellet Fm., Norway (Butterfield et al., 1994) 21
		~811-716.5 Ma, Alinya Fm., Australia (Riedman and Porter, 2016) 22
		~800-750 Ma, Chichkan Fm., Kazakhstan (Sergeev and Schopf, 2010) 23
		800-700 Ma, Draken Conglomerate Fm., Norway (Knoll et al., 1991) 24
		780-740 Ma, Chuar Gr., USA (Porter and Riedman, 2016) 25
		>610->590 Ma, Scotia Gr., Norway (Knoll, 1992) 26



*Trachystrichos*  
*phaera botula*  
*Valeria*  
*lophostriata*  
*Vidaloppala* sp.



ACCEPTED MANUSCRIPT



1346 New organic-walled microfossil assemblage in the Atar/El Mreiti Group,  
1347 Mauritania.

1348 Microfossil assemblage in support of late Meso- to early Neoproterozoic (Tonian)  
1349 age.

1350 First record of unambiguous eukaryotes in 1.1 Ga Western Africa.

1351 Acanthomorphs (incl. *Trachyhystrichopshaera aimika*) and the occurrence of a  
1352 pylome.

1353 Biostratigraphic and paleogeographic global expansion of mid-Proterozoic  
1354 biosphere.

1355

1356